5

Magnetoionic theory 2. Rays and group velocity

5.1. Introduction

In ch. 4 we studied the propagation of a plane progressive radio wave in a cold homogeneous plasma and derived expressions for the two refractive indices. We then examined how they depend on the electron concentration N for various fixed values of the frequency ω and the angle Θ between the wave normal and the vector $\boldsymbol{Y}$. The present chapter deals with the same problem, and is concerned with the dependence of the refractive indices on Θ and on ω. It is necessary to examine situations where more than one progressive wave is present with different wave normal directions. It is therefore convenient now to introduce a new Cartesian coordinate system ξ, η, ζ with fixed axes, and with the ζ axis parallel to the vector $\boldsymbol{Y}$. The wave normal has polar angles Θ, Φ, with the ζ axis as the polar axis. It is convenient to think of the refractive index as a vector $\boldsymbol{n}$ with magnitude n and in the direction of the wave normal. Thus $\boldsymbol{n}$ has the Cartesian components

$$n_\xi = n\sin\Theta\cos\Phi, \quad n_\eta = n\sin\Theta\sin\Phi, \quad n_\zeta = n\cos\Theta. \tag{5.1}$$

For any one of the plane waves studied here all field components depend on ξ, η, ζ only through an exponential factor which may be written in any of the forms

$$\begin{aligned}&\exp\{-\mathrm{i}k(\xi n_\xi + \eta n_\eta + \zeta n_\zeta)\} = \exp(-\mathrm{i}k\boldsymbol{n}\cdot\boldsymbol{g})\\ &\quad = \exp\{-\mathrm{i}kn(\xi\sin\Theta\cos\Phi + \eta\sin\Theta\sin\Phi + \zeta\cos\Theta)\}.\end{aligned} \tag{5.2}$$

where $\boldsymbol{g}$ is the vector (ξ, η, ζ). The dispersion relation (4.47) or (4.51) or (4.63) or (4.64) shows that n depends only on Θ and not on Φ. Thus let

$$n_\gamma = n\sin\Theta = (n_\xi^2 + n_\eta^2)^{\frac{1}{2}} \tag{5.3}$$

so that

$$n^2 = n_\gamma^2 + n_\zeta^2. \tag{5.4}$$

If these are inserted in (4.63) they give for the dispersion relation

$$\begin{aligned}&\tfrac{1}{2}(\varepsilon_1 + \varepsilon_2)n_\gamma^4 + \varepsilon_3 n_\zeta^4 + n_\gamma^2 n_\zeta^2\{\tfrac{1}{2}(\varepsilon_1 + \varepsilon_2) + \varepsilon_3\}\\ &\quad - n_\gamma^2\{\tfrac{1}{2}(\varepsilon_1 + \varepsilon_2)\varepsilon_3 + \varepsilon_1\varepsilon_2\} - n_\zeta^2(\varepsilon_1 + \varepsilon_2)\varepsilon_3 + \varepsilon_1\varepsilon_2\varepsilon_3 = 0.\end{aligned} \tag{5.5}$$

This is a quadratic either for n_γ^2 or for n_ζ^2, and may be solved to give one of these quantities in terms of the other. These solutions are useful in some problems; see, for example, Al'pert, Budden, Moiseyev and Stott (1983). The form (5.5) can also be written

$$\tfrac{1}{2}n_\gamma^2\left(\frac{1}{n^2-\varepsilon_1}+\frac{1}{n^2-\varepsilon_2}\right)+n_\zeta^2\frac{1}{n^2-\varepsilon_3}=1. \tag{5.6}$$

5.2. Refractive index surfaces

Consider now a system of Cartesian coordinates n_ξ, n_η, n_ζ with axes parallel to the ξ, η, ζ axes of ordinary space. It defines a three-dimensional space called 'refractive index space', and in it we use the same polar angles Θ, Φ, as in ordinary space. Let a surface be constructed such that the radius from the origin to any point on it has the direction of the wave normal and length equal to the refractive index n. For any cold plasma there are two such surfaces, one for the ordinary and one for the extraordinary wave. These surfaces are called 'refractive index surfaces'. For a magnetoplasma the shape is shown by a cross section in any plane Φ = constant, and it is simply the curve $n(\Theta)$ in polar coordinates with radius n and angle Θ. Some examples are given figs. 5.4–5.13.

The main properties of these surfaces will now be listed. They are given for a collisionless plasma and mainly for the electron plasma in which X and Y are held constant, but some results for the more general plasma, with ions, are included too. Because of the symmetry property (2) it is sufficient to consider only the range $0<\Theta<\frac{1}{2}\pi$.

(1) Since $n(\Theta)$ is independent of Φ, each surface is a surface of revolution about the n_ζ axis.

(2) Since $n(\pi-\Theta)=n(\Theta)$, the plane $\Theta=\pi/2$, that is $n_\zeta=0$, is a plane of symmetry.

(3) When $X\to 0$ the plasma goes over to free space and both values of n tend to unity. The two refractive index surfaces tend to unit spheres.

(4) For an isotropic plasma there is only one value of n and it is independent of Θ. The refractive index surface is a sphere of radius n.

(5) The square root in (4.48), or (4.67) with $U=1$, is never zero when Θ is not 0 or $\frac{1}{2}\pi$, so the two refractive index surfaces never cross. If collisions are allowed for the refractive index surface is a complex surface. The two complex ns are equal where $\Theta=\Theta_t$ given by (4.96). This defines a real 'transition cone' in refractive index space. It is analogous to the optic axes of a crystal; see § 5.5. (Davids, 1953.)

(6) The equation (5.5) or (5.6) of the system of refractive index surfaces is of fourth degree in n_ξ, n_η, n_ζ. Thus no straight line in refractive index space can cut the two surfaces in more than four points. This applies in particular to a straight line through the origin. Hence for any given Θ there can at most be two real positive

values of n. Each polar curve $n(\Theta)$ is single valued, continuous except where $n \to \infty$, and cannot have loops or cusps; see (11) below.

(7) When $X \to 1$ parts of the refractive index surfaces shrink down towards segments of the line $\Theta = 0$. The behaviour is shown in figs. 5.4, 5.5, 5.9–5.11. In the limit $X = 1$ the two surfaces touch at the points $n = \pm\{Y/(Y+1)\}^{\frac{1}{2}}$, $\Theta = 0$, and also at the points $n = \pm\{Y/(Y-1)\}^{\frac{1}{2}}$, $\Theta = 0$. The last two are real only if $Y > 1$. This defines four points in refractive index space, known as window points. See §§ 4.11, 4.12.

(8) One refractive index surface is a sphere in the three following cases:

(a) Window frequency, $\varepsilon_3 = 0$, $n^2 = 2\varepsilon_1\varepsilon_2/(\varepsilon_1 + \varepsilon_2)$ (in electron plasma $X = 1$, $n^2 = 1$),

(b) Crossover $\varepsilon_1 = \varepsilon_2 = n^2$,

(c) $\varepsilon_1 = \varepsilon_3 = n^2$.

Only the first of these cases can occur in an electron plasma. In the terrestrial plasmas the third case only occurs where ε_3 is negative so n is imaginary, and a fourth case $\varepsilon_2 = \varepsilon_3$ cannot occur at all.

(9) A refractive index surface does not go in to zero radius for any Θ, unless $X = 1 \pm Y$, (ε_1 or ε_2 zero), and then one value of n is zero for all Θ.

(10) If ε_1 is small and positive, the equation for one refractive index surface is, from (4.68)

$$n^2 \approx 2\varepsilon_1/(1 + \cos^2\Theta) \approx 2(1 - X + Y)/\{(1 + Y)(1 + \cos^2\Theta)\} \qquad (5.7)$$

where the second form is for the collisionless electron plasma. The surface is approximately a small ellipsoid. A similar result applies when ε_2 is small and positive; ε_1 is replaced by ε_2 and the sign of Y is changed in (5.7). Thus, near cut-off, if n is to be real, the element ε_1 or ε_2 that is zero at the cut-off must now be positive, which means that the frequency must slightly exceed the cut-off frequency (compare § 5.7 item (5)), or equivalently, X must be slightly less than its value at cut-off.

(11) One value of n is infinite where

$$\Theta = \Theta_r, \quad \cos^2\Theta_r = (Y^2 + X - 1)/XY^2. \qquad (5.8)$$

This defines a cone in refractive index space known as a resonance cone. There cannot be more than one. It can occur for real Θ only if

$$Y < 1 \quad \text{and} \quad 1 - Y^2 \leqslant X \leqslant 1 \qquad (5.9)$$

or

$$Y > 1 \quad \text{and} \quad X \geqslant 1 (\text{or } X \leqslant 1 - Y^2). \qquad (5.10)$$

The condition in brackets is for negative X and of no great practical importance, but see figs. 4.5, 4.6. When (5.10) holds, the n that is infinite for $\Theta = \Theta_r$ is real for $\Theta < \Theta_r$ and the cone $\Theta = \Theta_r$ is called a forward resonance

cone. This occurs for the whistler mode, §§ 4.12, 13.8. When (5.9) holds, the n that is infinite for $\Theta = \Theta_r$ is real for $\Theta > \Theta_r$ and the cone $\Theta = \Theta_r$ is called a reversed resonance cone. This occurs for the Z-mode, §§ 4.11, 16.8. It can be shown, from the dispersion relation (4.63) or (4.64) or from its solution (4.51) or (4.68) respectively that near resonance

$$n \approx K \sin^{-\frac{1}{2}}(\Theta - \Theta_r) \tag{5.11}$$

where K is a constant.

(12) By differentiating (4.65) with respect to Θ and using (4.66) it can be shown that

$$\frac{1}{n}\frac{dn}{d\Theta} = \pm\tfrac{1}{2}\sin\Theta\cos\Theta\, Y(n^2-1)\{\tfrac{1}{4}Y^2\sin^4\Theta + (1-X)^2\cos^2\Theta\}^{-\frac{1}{2}} \tag{5.12}$$

where the + sign applies for the ordinary wave and the − sign for the extraordinary wave. This shows that $dn/d\Theta$ is zero when $\Theta = 0$ or $\frac{1}{2}\pi$. The Appleton–Lassen formula (4.48) shows that when $X \neq 0$, n can never be 1 unless $X = 1$, and then one value of n is 1 for all Θ, so the refractive index surface is the unit sphere. Apart from this case and, for the more general plasma, cases (a), (b), (c) of item (8) above, $dn/d\Theta$ is never zero when $\Theta \neq 0$, and $\neq \frac{1}{2}\pi$. Thus in the range of Θ where it is real and positive, n is a monotonic function of Θ. This proves the statement in § 4.11 that the continuous curves of figs. 4.3, 4.5, 4.6 must lie within the shaded regions as shown. This monotonic property also holds for the general plasma with ions allowed for; see problem 5.4.

In some problems it is necessary to know the curvature of the refractive index surface. It is not needed for the topics discussed later in this book, but some formulae and references are given here for completeness. A full discussion has been given by Stott (1983).

Budden and Hugill (1964) used the Gaussian curvature, that is, the product of the two principal curvatures, and gave formulae for it for a collisionless electron plasma. The curvature of the curve $n(\Theta)$ is proportional to d^2n_ζ/dn_γ^2 and formulae for this were given by Al'pert, Budden, Moiseyev and Stott (1983).

A point of inflection of the curve $n(\Theta)$ may occur at an angle $\Theta = \Theta_s$ which defines a cone called a Storey cone because Storey (1953) drew attention to one of the most important occurrences of it, in the theory of whistlers. The condition is $d^2n_\zeta/dn_\gamma^2 = 0$ from which Θ_s can be found by solving an equation of degree six. This was given by Clemmow and Mullaly (1955) for an electron plasma, and by Budden and Stott (1980) and Stott (1983) for the more general plasma. If the curve $n(\Theta)$ is concave towards the origin when $\Theta < \Theta_s$, the cone $\Theta = \Theta_s$ is called a (forward) Storey cone, and if it is convex towards the origin for $\Theta < \Theta_s$ the cone is called a reversed Storey cone.

Stott (1983) has shown that for any one quadrant $0 < \Theta < \frac{1}{2}\pi$ there cannot be

more than two values of Θ_s, and when there are two they must occur in the same refractive index surface, that is both ordinary or both extraordinary.

The curvature when $\Theta = 0$ is most easily found from the series expansion (4.102) or (4.101) and is given, for one wave, by

$$(\mathrm{d}^2 n_\zeta/\mathrm{d}n_\gamma^2)_0 = -\frac{1}{2}\frac{\varepsilon_1+\varepsilon_3}{\varepsilon_3\varepsilon_1^{\frac{1}{2}}} = \frac{Y(2-X)-2(X-1)}{2(X-1)(1+Y)}\left(\frac{1+Y}{1+Y-X}\right)^{\frac{1}{2}} \tag{5.13}$$

where subscript 0 denotes the value at $\Theta = 0$. Thus Θ_s is zero when

$$\varepsilon_1 + \varepsilon_3 = 0 \tag{5.14}$$

(Walker, 1977b) or, for the electron plasma, when

$$Y = 2(X-1)/(2-X), \quad X = 2(1+Y)/(2+Y). \tag{5.15}$$

(Clemmow and Mullaly, 1955). This condition gives a transition in the C.M.A. diagram, described later, §5.4. For the other wave, ε_1 is replaced by ε_2, or equivalently the sign of Y is reversed; see (5.50).

For $\Theta = \frac{1}{2}\pi$ the curvature of the refractive index surface for the ordinary wave is given, in a similar way, from the expansion (4.104) or (4.103), by

$$(\mathrm{d}^2 n_\gamma/\mathrm{d}n_\zeta^2)_\mathrm{A} = \varepsilon_3^{\frac{1}{2}} G/J = -(1-X)^{\frac{1}{2}} \tag{5.16}$$

and for the extraordinary wave, from the expansion (4.106) or (4.105) by

$$\begin{aligned}(\mathrm{d}^2 n_\gamma/\mathrm{d}n_\zeta^2)_\mathrm{B} &= \frac{\varepsilon_1\varepsilon_2(\varepsilon_1+\varepsilon_2)-\varepsilon_3(\varepsilon_1^2+\varepsilon_2^2)}{J\{2\varepsilon_1\varepsilon_2(\varepsilon_1+\varepsilon_2)\}^{\frac{1}{2}}} \\ &= \frac{X^2+Y^2-1}{[(1-X-Y^2)\{(1-X)^2-Y^2\}]^{\frac{1}{2}}}\end{aligned} \tag{5.17}$$

where subscripts A, B denote the values at $\Theta = \frac{1}{2}\pi$ for the ordinary and extraordinary waves respectively. The curvature (5.16) is independent of Y but is not the same as the curvature $-n^{-1} = -(1-X)^{-\frac{1}{2}}$ for an isotropic plasma. There is a discontinuity in the curvature of both refractive index surfaces at $\Theta = \frac{1}{2}\pi$ when Y changes from zero to a small non-zero value.

The curvature (5.17) is zero when

$$\varepsilon_1\varepsilon_2(\varepsilon_1+\varepsilon_2) - \varepsilon_3(\varepsilon_1^2+\varepsilon_2^2) = 0 \tag{5.18}$$

(Walker, 1977b), or for the electron plasma

$$X^2 + Y^2 = 1 \tag{5.19}$$

(Clemmow and Mullaly, 1955). This condition gives a transition in the C.M.A. diagram; see §5.6. Again (5.17), when $Y = 0$, is not the same as for an isotropic plasma. There is a discontinuity of behaviour when Y changes from zero to a non-zero value.

When collisions are allowed for, all three components of $\boldsymbol{n}$ are in general complex

and refractive index space is a three-dimensional complex space, that requires six real dimensions to represent it. The refractive index surfaces are complex surfaces in this space, though they are still surfaces of revolution about the n_ζ axis. Thus they can be studied by using a cross section plane $\Phi =$ constant. If only real values of Θ are of interest it is then useful to plot the polar diagrams of $\mu(\Theta)$ and $\chi(\Theta)$ where $n = \mu - i\chi$. This has been done, for example, by Jones (1972). In many problems, however, we need to consider complex values of Θ. There is then no simple graphical way of representing the refractive index surfaces and we have to rely on algebraic methods. The topic is discussed again later, § 14.12.

5.3. The ray. Ray surfaces

We now ask: what is the direction of the time averaged Poynting vector $\boldsymbol{\Pi}_{av}$ for a progressive plane wave in a homogeneous loss free plasma? The answer is that it is normal to the refractive index surface (Al'pert, 1948).

The proof is as follows. For the plane wave with real refractive index vector $\boldsymbol{n}$, Maxwell's third and fourth equations in the form (2.44) give, on cancellation of a factor $-ik$;

$$\boldsymbol{n} \wedge \boldsymbol{E} = \mathscr{H} \tag{5.20}$$

$$\boldsymbol{n} \wedge \mathscr{H} = -\varepsilon_0^{-1}\boldsymbol{D}. \tag{5.21}$$

Consider a second plane wave whose refractive index vector is $\boldsymbol{n} + \delta\boldsymbol{n}$ where $\delta\boldsymbol{n}$ is infinitesimally small. Let the fields be $\boldsymbol{E} + \delta\boldsymbol{E}$, $\mathscr{H} + \delta\mathscr{H}$. Then (5.20), (5.21) may be differentiated to give

$$\boldsymbol{n} \wedge \delta\boldsymbol{E} + \delta\boldsymbol{n} \wedge \boldsymbol{E} = \delta\mathscr{H} \tag{5.22}$$

$$\boldsymbol{n} \wedge \delta\mathscr{H} + \delta\boldsymbol{n} \wedge \mathscr{H} = -\varepsilon_0^{-1}\delta\boldsymbol{D}. \tag{5.23}$$

Now take the scalar product of (5.22) with $\mathscr{H}^*$ and on the left hand side use the permutation property for the product of three vectors $\boldsymbol{a}\cdot(\boldsymbol{b} \wedge \boldsymbol{c}) = \boldsymbol{b}\cdot(\boldsymbol{c} \wedge \boldsymbol{a}) = \boldsymbol{c}\cdot(\boldsymbol{a} \wedge \boldsymbol{b})$. Then

$$\delta\boldsymbol{E}\cdot(\mathscr{H}^* \wedge \boldsymbol{n}) + \delta\boldsymbol{n}\cdot(\boldsymbol{E} \wedge \mathscr{H}^*) = \mathscr{H}^*\cdot\delta\mathscr{H} \tag{5.24}$$

Take the scalar product of (5.23) with $\boldsymbol{E}^*$ and permute the terms on the left in a similar way. Then

$$\delta\mathscr{H}\cdot(\boldsymbol{E}^* \wedge \boldsymbol{n}) - \delta\boldsymbol{n}\cdot(\boldsymbol{E}^* \wedge \mathscr{H}) = -\varepsilon_0^{-1}\boldsymbol{E}^*\cdot\delta\boldsymbol{D}. \tag{5.25}$$

For the vector products in the first terms of (5.24), (5.25) use the complex conjugates of (5.21), (5.20) respectively. Subtract the two equations and rearrange. This gives:

$$4\delta\boldsymbol{n}\cdot\boldsymbol{\Pi}_{av} - \varepsilon_0^{-1}(\boldsymbol{E}^*\cdot\delta\boldsymbol{D} - \boldsymbol{D}^*\cdot\delta\boldsymbol{E}) = 0 \tag{5.26}$$

where (2.63) for $\boldsymbol{\Pi}_{av}$ has been used. Now use the subscript notation form (2.54) for $\boldsymbol{D}$. Since the plasma is loss-free, $\boldsymbol{\varepsilon}$ is Hermitian, (2.56). Then

$$\boldsymbol{D}^*\cdot\delta\boldsymbol{E} = \varepsilon_0\varepsilon_{ij}^* E_j^* \delta E_i = \varepsilon_0 E_j^* \varepsilon_{ji}\delta E_i = \boldsymbol{E}^*\cdot\delta\boldsymbol{D}. \tag{5.27}$$

This shows that the second term of (5.26) is zero, so that

$$\delta \boldsymbol{n} \cdot \boldsymbol{\Pi}_{\mathrm{av}} = 0. \tag{5.28}$$

Now $\delta \boldsymbol{n}$ must lie in the refractive index surface, and $\boldsymbol{\Pi}_{\mathrm{av}}$ is perpendicular to all possible $\delta \boldsymbol{n}$s with this property. Hence $\boldsymbol{\Pi}_{\mathrm{av}}$ is normal to the surface.

A result equivalent to this will now be derived in a different way. Suppose that there is a point source at the origin of coordinates. If the medium were homogeneous the source would emit a wave whose wavefronts are outward travelling spheres. We need to find the shape of the wavefronts in an anisotropic medium. In any plane $\zeta = \text{constant}$, each field component is a function of ξ, η which can be expressed as a two-dimensional Fourier integral, whose integrand contains a factor $\exp\{-\mathrm{i}(\xi\kappa_\xi + \eta\kappa_\eta)\}$, where $\kappa_\xi = kn_\xi$, $\kappa_\eta = kn_\eta$. But this is the same as the ξ and η dependence of the field (5.2) of a plane wave. Thus the fields in the chosen plane $\zeta = \text{constant}$ are a doubly infinite spectrum of plane waves. The fields in any other plane can now be found by using the known properties of the plane waves as derived in the preceding chapter. The dispersion relation (5.3)–(5.5) shows that there are two different possible values of n_ζ. Thus the plane wave spectrum can be resolved into two separate systems, for the ordinary and extraordinary waves. We confine attention to one of these systems. Then any field component in the wave of that system emitted by the point source is given by

$$F(\xi, \eta, \zeta) = \int_{-\infty}^{\infty} \int_{-\infty}^{\infty} A(n_\xi, n_\eta) \exp\{-\mathrm{i}k(\xi n_\xi + \eta n_\eta + \zeta n_\zeta)\} \, \mathrm{d}n_\xi \, \mathrm{d}n_\eta. \tag{5.29}$$

The exponential represents a plane wave, and (5.29) is said to express the field as an 'angular spectrum of plane waves'. For a full description see Clemmow (1966) and for an example of its use see Al'pert, Budden, Moiseyev and Stott (1983). The function A is a 'slowly varying' function of n_ξ, n_η (see § 9.6). The exponential is rapidly varying when ξ, η and ζ are large. In the present discussion it is adequate to treat A as constant for small ranges of n_ξ, n_η, n_ζ. The quantity

$$\varphi = k(\xi n_\xi + \eta n_\eta + \zeta n_\zeta) \tag{5.30}$$

is called the phase of the integrand. The integral (5.29) is the sum of numerous complex numbers whose phases in general are different so that there is partial cancellation and the sum is not large. But there can be regions of the n_ξ–n_η plane where the phase does not change much for small changes $\delta n_\xi, \delta n_\eta$ and the resulting small change δn_ζ derived from the dispersion relation. From these regions the contributions to the integral are large. Thus the main contributions to (5.29) come from regions where the phase is stationary for small variations $\delta n_\xi, \delta n_\eta$. We seek a refractive index vector $\boldsymbol{n}$ such that

$$\delta\varphi = 0: \quad \xi \delta n_\xi + \eta \delta n_\eta + \zeta \delta n_\zeta = 0\,. \tag{5.31}$$

Now any $\delta \boldsymbol{n}$ lies in the refractive index surface, so that the vector $\boldsymbol{g} = \xi, \eta, \zeta$ must be

normal to the refractive index surface and $\boldsymbol{n}$ must be found to achieve this. The vector $\boldsymbol{g}$ is represented by a line drawn out from the origin in a fixed direction, and known as the 'ray'. The more formal definition of the term 'ray' is discussed later, §§ 10.1, 14.1–14.3.

The particular vector $\boldsymbol{n}$ where (5.31) is exactly satisfied is called the predominant $\boldsymbol{n}$ of the spectrum in (5.29). This integral can be evaluated by the method of steepest descents (§ 9.6) to give an expression for $F(\boldsymbol{g})$ containing a factor $\exp(-i\boldsymbol{k}\boldsymbol{n}\cdot\boldsymbol{g})$. Thus at points on a given ray $\boldsymbol{g}$, the direction of $\boldsymbol{n}$ is the predominant wave normal on that ray. It is usually called simply the 'wave normal'. It is different for different rays. Because the refractive index surface is a surface of revolution about the ζ axis, it follows that the ray, the wave normal and the ζ axis are coplanar. Let β be the angle between the ray and the ζ axis so that

$$\alpha = \Theta - \beta \tag{5.32}$$

is the angle between the ray and the wave normal. Then it follows by a geometrical construction shown in fig. 5.1 that

$$\tan\alpha = \frac{1}{n}\frac{\partial n}{\partial\Theta}. \tag{5.33}$$

An expression for this, for an electron plasma without collisions, has already been given at (5.12).

Fig. 5.1. Cross section of refractive index surface by a plane containing the direction of the earth's magnetic field. CX and CA are the normal and tangent, respectively, at the point C. The line OC, of length n, is parallel to the wave normal. CB is perpendicular to OA and has length $\approx n\delta\Theta$.

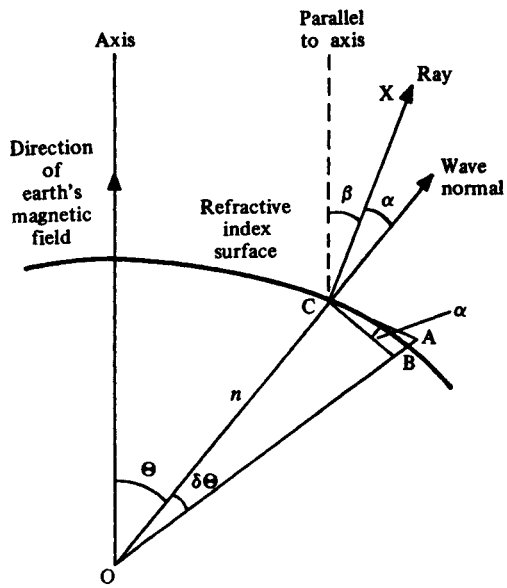

The contributing plane waves in (5.29) whose refractive index vectors are close to $\boldsymbol{n}$ have nearly equal phases and add together constructively at points on the ray, but, except when $\alpha = 0$, not at points on a wave normal through the origin. The velocity of a wave front in the direction of the wave normal is

$$v = c/n \tag{5.34}$$

and is called the wave velocity. The velocity of a point where the wave front intersects a ray is

$$v \sec \alpha = c/(n \cos \alpha) = V = c/\mathscr{M} \tag{5.35}$$

and is called the ray velocity. It is the magnitude of a vector $\boldsymbol{V}$ in the direction of the ray and we have seen, at (5.28), that it is also the direction of the time averaged Poynting vector, $\boldsymbol{\Pi}_{\mathrm{av}}$. The product $n \cos \alpha = \mathscr{M}$ is called the 'ray refractive index', and is used in §§13.7, 14.6.

Now a surface is constructed whose points are given by the vector $\boldsymbol{V}$ drawn from the origin. It is called the 'ray surface'. A point on a ray travelling outwards with velocity $\boldsymbol{V}$ is a point where the phase stays constant as the wave travels. This applies for all rays and the locus of these points is the surface where the phase is constant. In other words it is the wave front of the wave field going out from the point source at the origin. Thus the ray surface gives the shape of the wave front going out from a point source (Budden, 1961a; Walker, 1977a). The normal to the local wave front is the wave normal and has the direction of $\boldsymbol{n}$. Thus the predominant refractive index vector $\boldsymbol{n}$ is normal to the ray surface.

5.4. Properties of ray surfaces

The ray surface can be plotted by first choosing a value of the wave normal direction Θ and computing $n(\Theta)$ from the dispersion relation. Then α is found from (5.33) or equivalently (5.12), β from (5.32) and V from (5.35). This is a possible method for computing, but β is not at first known. A succession of values of Θ must be used until all the required values of β have been covered. For a plasma with collisions allowed for, Θ is complex and the process may be laborious.

A radio signal does not, in general, travel in the direction of the wave normal, but along the ray, and in many practical problems it is the ray direction β that is given, but the wave normal direction Θ is at first unknown so that the dispersion relation cannot immediately be used to find n or α or V. A formula is required that gives these quantities when β, but not Θ, is given. This formula has been given, for an electron plasma, by Budden and Daniell (1965), and for the more general plasma by Budden and Stott (1980) and Stott (1983). It is an equation for finding n^2 and is of degree six. It is not used in this book, except in the present section, and it is too long to be worth quoting here. It is given in full in the references cited above. Stott (1983) has shown that, for a loss-free plasma, at most four of the solutions n^2 can be real and positive,

and that, for all β, one of the two ray surfaces cannot have more than one real positive value of n^2. The equation is useful for finding some of the properties of ray surfaces. One of its main uses is for finding the saddle points for integrals like (5.29) representing an angular spectrum of plane waves; see Al'pert, Budden, Moiseyev and Stott (1983).

The main properties of ray surfaces will now be listed. As for refractive index surfaces, § 5.2, they are given for a collisionless plasma and mainly for the electron plasma, but some results for the more general plasma are included. The ray surfaces are surfaces in a space with coordinates V_ξ, V_η, V_ζ and axes parallel to the ξ, η, ζ axes of ordinary space. The ray vector V makes an angle β with the V_ζ axis and has azimuth angle Φ, the same Φ as for the wave normal. Because of the symmetry property (2) it is sufficient to consider only the range $0 \leqslant \beta \leqslant \frac{1}{2}\pi$.

(1) $V(\beta)$ is independent of Φ. Each ray surface is a surface of revolution about the V_ζ axis.

(2) $V(\pi - \beta) = V(\beta)$. The plane $\beta = \frac{1}{2}\pi$ is a plane of symmetry.

(3) In free space both ray surfaces are spheres of radius c.

(4) For an isotropic plasma both ray surfaces are spheres of radius c/n.

(5) A radius drawn out from the origin can cross a ray surface in one, two or three points. For examples see figs. 5.6, 5.9–5.11.

(6) To each point V on a ray surface there is a corresponding point $\boldsymbol{n}$ on the refractive index surface. From (5.34), (5.35) it follows that

$$\boldsymbol{V}\cdot\boldsymbol{n} = Vn\cos\alpha = V_\xi n_\xi + V_\eta n_\eta + V_\zeta n_\zeta = c. \tag{5.36}$$

Points with this property are said to be reciprocal with respect to the sphere of radius c.

(7) The normal to the ray surface at $\boldsymbol{V}$ is parallel to the corresponding $\boldsymbol{n}$. The normal to the refractive index surface at $\boldsymbol{n}$ is parallel to the corresponding $\boldsymbol{V}$.

(8) Cut-off occurs when $\varepsilon_1 \to 0$ or $\varepsilon_2 \to 0$. Consider the first of these. When ε_1 is very small the refractive index surface is approximately the small ellipsoid (5.7) whence it can be shown from (5.33), (5.32), (5.35) that

$$\cos^2\beta \approx 4\cos^2\Theta/(1 + 3\cos^2\Theta), \quad V^2 \approx \tfrac{1}{2}c^2/\{\varepsilon_1(1 - \tfrac{1}{2}\cos^2\beta)\}. \tag{5.37}$$

Thus the ray surface is a large ellipsoid and, at exact cut-off, $V \to \infty$ for all β. The behaviour when $\varepsilon_2 \to 0$ is exactly similar.

(9) Near a resonance, $\Theta \to \Theta_r$, the refractive index is given by (5.11) which shows, from (5.33) that

$$\tan\alpha = -\tfrac{1}{2}\cot(\Theta - \Theta_r) \tag{5.38}$$

so that $\alpha \to \pm\pi/2$ and $\beta \to \beta_r = \Theta_r - \alpha$. Thus $\cos\alpha \to 0$. Although $n \to \infty$, the product

$$n\cos\alpha \approx 2K\sec(\Theta - \Theta_r)\sin^{\frac{1}{2}}(\Theta - \Theta_r) \tag{5.39}$$

tends to zero. Hence $V \to \infty$. The angle $\beta = \beta_r$ defines a resonance cone in the ray surface. Suppose that β_r is in the quadrant $0 < \beta_r < \frac{1}{2}\pi$. Then two cases can occur. First Θ_r may be in the range $-\frac{1}{2}\pi < \Theta_r < 0$. Then V is real when $\beta < \beta_r$ and n is real when $\Theta < |\Theta_r|$. The resonance cones are forward resonance cones; see item (11) of §5.2. See figs. 5.5, 5.6 for examples. Second Θ_r may be in the range $\frac{1}{2}\pi < \Theta_r < \pi$. Then V is real for $\beta > \beta_r$ and n is real for $\pi - \Theta_r < \Theta < \Theta_r$. The resonance cones are reversed resonance cones. See figs. 5.8, 5.9 for examples.

(10) When $\beta = 0$ and V is real, one value of Θ is 0, and $n = c/V$. There may be other real values of Θ, n and V; see for example figs. 5.6, 5.11. Similarly when $\beta = \frac{1}{2}\pi$ and V is real, one value of Θ is $\frac{1}{2}\pi$ and $n = c/V$. Again there may be other real values of Θ, n and V; see for example fig. 5.9.

(11) The ray and wave normal are parallel, that is $\alpha = 0$, when $\Theta = \beta = 0$ and $\Theta = \beta = \frac{1}{2}\pi$ as in (10). They are parallel for all $\beta = \Theta$ when the refractive index surface is a sphere as in (3), (4) above or in item (8) of § 5.2. There are no other cases where they are parallel.

(12) The ray direction β, normal to the refractive index surface, attains a maximum or minimum value when the point $\boldsymbol{n}$ on the refractive index surface moves through a point of inflection, $\Theta = \Theta_s$. Here let $\beta = \beta_s$. The value of Θ gives the direction of the normal to the ray surface and here changes smoothly and continuously. It follows that the ray surface has a cusp where $\beta = \beta_s$. This defines a Storey cone in the ray surface if V is real where $\beta < \beta_s$ and a reversed Storey cone if V is real where $\beta > \beta_s$. The angles β_s and Θ_s, may have opposite signs (see, for example, fig. 5.11) or the same sign (see, for example, figs. 5.6, 5.9, 5.10).

5.5. Crystal optics

The properties of a plane progressive radio wave in a homogeneous magnetoplasma are similar in some respects to those of an electromagnetic wave of optical frequency in a crystal, and it is useful to make a brief comparison.

For many purposes a crystalline medium can be treated as a non-magnetic dielectric. Spatial dispersion effects can sometimes be important and they give rise to 'optical activity' (see problem 13.2) but here they are neglected. For most crystals energy losses are negligible and the dielectric tensor $\boldsymbol{\varepsilon}$ is real and symmetric. It is then possible to choose a Cartesian coordinate system ξ, η, ζ with real axes, so that $\boldsymbol{\varepsilon}$ is diagonal with real positive elements $\varepsilon_a, \varepsilon_b, \varepsilon_c$ and the axes are chosen so that $\varepsilon_a < \varepsilon_b < \varepsilon_c$.

If $\mathscr{H}$ is eliminated from Maxwell's equations (2.44) they give

$$\operatorname{curl}\operatorname{curl} \boldsymbol{E} = k^2 \varepsilon_0^{-1} \boldsymbol{D} = k^2 \boldsymbol{\varepsilon} \boldsymbol{E}. \tag{5.40}$$

For a plane progressive wave with refractive index vector $\boldsymbol{n} = (n_\xi, n_\eta, n_\zeta)$. We may use

curl $\boldsymbol{E} = -\mathrm{i}k\boldsymbol{n} \wedge \boldsymbol{E}$ whence (5.40) gives

$$\begin{pmatrix} n_\xi^2 - n^2 + \varepsilon_a & n_\xi n_\eta & n_\xi n_\zeta \\ n_\xi n_\eta & n_\eta^2 - n^2 + \varepsilon_b & n_\eta n_\zeta \\ n_\xi n_\zeta & n_\eta n_\zeta & n_\zeta^2 - n^2 + \varepsilon_c \end{pmatrix} \begin{pmatrix} E_\xi \\ E_\eta \\ E_\zeta \end{pmatrix} = 0. \tag{5.41}$$

For solutions to exist, the determinant of the matrix must be zero and this gives the dispersion relation. It can be shown that this leads to

$$\frac{n_\xi^2}{n^2 - \varepsilon_a} + \frac{n_\eta^2}{n^2 - \varepsilon_b} + \frac{n_\zeta^2}{n^2 - \varepsilon_c} = 1. \tag{5.42}$$

This is the equation of the refractive index surfaces. Its properties are well known and are described in textbooks of optics; see for example Born and Wolf (1970, ch. 14) or Lipson and Lipson (1969, § 5.4). It should be compared with (5.6) which is the analogous form for a magnetoplasma.

If $\boldsymbol{n}$ has a given real direction, (5.42) is a quadratic for n^2 which always has two real positive solutions. There is no cut-off and no resonance (compare § 5.2 items (9), (10), (11)). Any radius drawn outwards from the origin cuts the refractive index surfaces in two real points. It can be shown that the wave polarisations of the two waves are linear. As in a magnetoplasma, $\boldsymbol{E}$ may have a component parallel to the wave normal.

The origin is a centre of symmetry of the refractive index surfaces, and the planes $n_\xi = 0, n_\eta = 0, n_\zeta = 0$ are planes of symmetry, called principal planes. But the surfaces are not surfaces of revolution about any axis. In each principal plane the cross section of the surfaces is a circle and an ellipse. For $n_\zeta = 0$ the circle is entirely outside the ellipse, and for $n_\xi = 0$ it is entirely inside the ellipse. For the plane $n_\eta = 0$, equation (5.42) gives

$$(n^2 - \varepsilon_b)\left(\frac{n_\xi^2}{\varepsilon_c} + \frac{n_\zeta^2}{\varepsilon_a} - 1\right) = 0. \tag{5.43}$$

The first factor gives the circle of radius $\varepsilon_b^{\frac{1}{2}}$ and the second gives the ellipse with major axis $\varepsilon_c^{\frac{1}{2}}$ and minor axis $\varepsilon_a^{\frac{1}{2}}$. These curves intersect at four points satisfying

$$\frac{n_\xi^2}{n_\zeta^2} = \tan^2 \Theta_w = \frac{\varepsilon_c(\varepsilon_b - \varepsilon_a)}{\varepsilon_a(\varepsilon_c - \varepsilon_b)}. \tag{5.44}$$

This defines four directions, one in each quadrant of the plane $n_\eta = 0$, that is $\Phi = 0$. They are called 'optic axes'. It can be shown that these are the only directions where the two values of n are equal. Near an optic axis the refractive index surfaces have the shape of two cones with their apices touching. The ray direction is normal to these cones and an infinite number of directions is possible, all lying in the surface of another cone. This gives the phenomenon of internal conical refraction; Born and Wolf (1970, p. 688). For a collisionless magnetoplasma there are no real optic axes.

The closest analogue to them is the transition cone $\Theta = \Theta_t$, § 5.2 item (5), in a plasma with collisions allowed for.

The ray velocity vector V is defined just as for a magnetoplasma. It is normal to the refractive index surface and satisfies (5.36). It can be shown that the equation of the ray surfaces is

$$\frac{V_\xi^2}{V^2 - c^2/\varepsilon_a} + \frac{V_\eta^2}{V^2 - c^2/\varepsilon_b} + \frac{V_\zeta^2}{V^2 - c^2/\varepsilon_c} = 1. \tag{5.45}$$

Thus their general geometrical properties are very similar to those for the refractive index, (5.42). In particular, in the plane $V_\eta = 0$ there are four directions, one in each quadrant, where the two values of V are equal, given by

$$\frac{V_\xi^2}{V_\zeta^2} = \tan^2\Theta_x = \frac{\varepsilon_b - \varepsilon_a}{\varepsilon_c - \varepsilon_b}. \tag{5.46}$$

These directions are called optic ray axes and are not the same as the optic axes. For an optic ray axis an infinite number of wave normal directions, that is normals to the ray surface, are possible all lying within the surface of a cone. This gives the phenomenon of external conical refraction; Born and Wolf (1970, p. 689).

Optic ray axes can occur in a magnetoplasma, and they are then always parallel to the earth's magnetic field. There are examples in figs. 5.6, 5.11, which show cross sections of the ray surface including the region where it has the form of two cones with touching apices. No radio experiment has been devised to show external conical refraction, though it would be possible in principle. But the field from a point source immersed in a plasma is enhanced in the direction of the optic ray axis, that is of the earth's magnetic field; Al'pert (1983); Al'pert, Budden, Moiseyev and Stott (1983).

A crystal in general has optic axes in two non-parallel directions, and is said to be biaxial. But if two of $\varepsilon_a, \varepsilon_b, \varepsilon_c$ are equal there is only one such direction, and the crystal is said to be uniaxial. We here suppose that $\varepsilon_b = \varepsilon_a$. Then (5.44) for the optic axes shows that $n_\xi = 0, \Theta_w = 0$ or π. Similarly (5.46) for the optic ray axes shows that $V_\xi = 0, \Theta_x = 0$ or π. The optic axes and the optic ray axes are both parallel to the n_ζ or V_ζ axis. On this axis the ray and the wave normal each have only one possible direction, parallel to the axis, so there is now no phenomenon of conical refraction. Equation (5.42) becomes:

$$(n^2 - \varepsilon_b)\{n_\xi^2 + n_\eta^2)/\varepsilon_c + n_\zeta^2/\varepsilon_b - 1\} = 0. \tag{5.47}$$

One refractive index surface is a sphere and the other is an ellipsoid outside it but touching it on the n_ζ axis. For the case $\varepsilon_b = \varepsilon_c > \varepsilon_a$ the optic axis would be the n_ξ axis and the ellipsoid would be inside the sphere, but otherwise the treatment is very similar. Equation (5.45) becomes

$$(V^2 - c^2/\varepsilon_b)\{(V_\xi^2 + V_\eta^2)\varepsilon_c + V_\zeta^2\varepsilon_b - c^2\} = 0. \tag{5.48}$$

One ray surface is a sphere and the other is an ellipsoid, inside it but touching it on the V_ζ axis.

A magnetoplasma is uniaxial when $\varepsilon_1 = \varepsilon_2$. This cannot happen exactly for an electron plasma, but it can happen for the more general collisionless magnetoplasma, always when ε_3 is negative. Then equation (5.6) for the refractive index surfaces is

$$(n^2 - \varepsilon_1)(n_\gamma^2/\varepsilon_3 + n_\zeta^2/\varepsilon_1 - 1) = 0. \tag{5.49}$$

One surface is a sphere of radius $\varepsilon_1^{\frac{1}{2}}$ and the other is a hyperboloid with resonances given by $\tan^2\Theta_r = -\varepsilon_3/\varepsilon_1$. Similarly one ray surface is a sphere and the other is a hyperboloid.

For the electron plasma it is sometimes useful to assume that the earth's magnetic field is large enough, or the frequency is small enough to make the approximation $Y \to \infty$. Then $\varepsilon_1 \approx \varepsilon_2 \approx 1$ and the medium is uniaxial. See § 19.3, and problem 4.7.

5.6. Classification of refractive index and ray surfaces. C.M.A. type diagrams

Refractive index surfaces can take various forms, depending, for example, on whether points of inflection and resonances are present. The forms depend on the particle concentrations N_e, N_i in the plasma, and on the frequency ω, and change when certain transition values of these parameters are crossed. It is useful to classify these forms of the refractive index surface. This was done for an electron plasma by Clemmow and Mullaly (1955) and by Allis (1959), who used diagrams now known as

Fig. 5.2. C.M.A. type diagram for the ordinary wave in a collisionless electron plasma. Table 5.1 gives the meanings of the symbols.

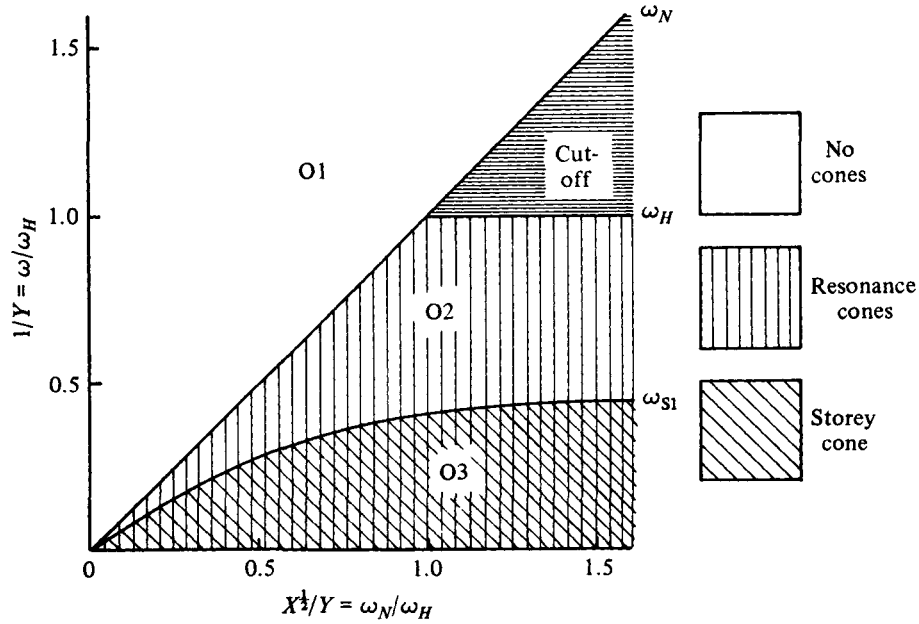

C.M.A. diagrams. When collisions are allowed for, refractive index surfaces are complex and cannot be simply described or classified. A collisional plasma is therefore classified by the real refractive index surfaces that it would have when the collisions are ignored.

In this section we shall consider only a collisionless electron plasma and we shall

Fig. 5.3. C.M.A. type diagram for the extraordinary wave in a collisionless electron plasma. Table 5.1 gives the meanings of the symbols.

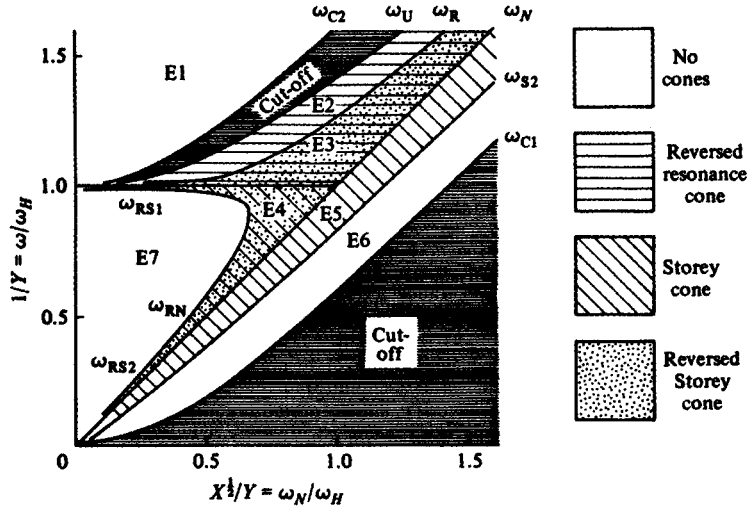

Fig. 5.4. Cross section by a plane $\phi =$ constant of the refractive index surfaces (left-hand figure) and ray surfaces (right-hand figure). The numbers by the curves are the values of X. In the left figure the curve $X = 0$ is the unit circle and in the right figure it is the circle of radius c. In figures where these circles are drawn as broken lines, they are not part of the system but are shown to give the scale. The same plan is used for figs. 5.5–5.13.

Region O1. Both refractive index surface and ray surface are concave towards the origin. When X is near to 1 the refractive index surface is a narrow cigar shaped surface. In the limit $X \to 1$ it shrinks to a segment of the line $\Theta = 0$ between the window points $n = \pm \{Y/(Y+1)\}^{\frac{1}{2}}$; §§ 4.11, 4.12, 5.2 item (7). In this example, $Y = 0.5$.

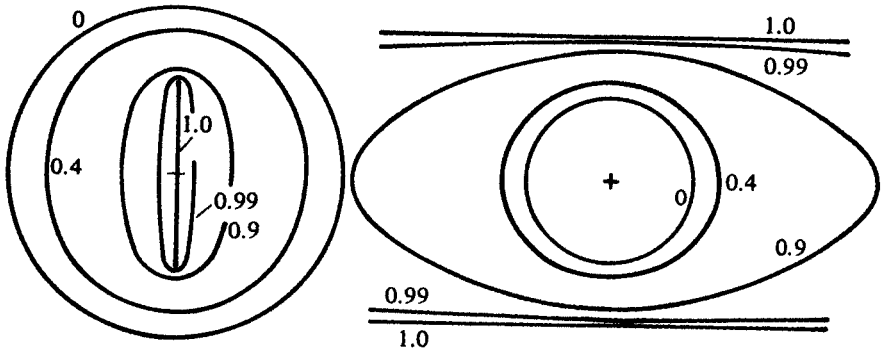

Table 5.1. *'No. of cones' applies to one quadrant* $0 < \Theta < \frac{1}{2}\pi$ or $0 < \beta < \frac{1}{2}\pi$

Region	n^2	Sign of $\partial n/\partial\Theta$	No. of Storey cones	No. of reversed Storey cones	No. of forward resonance cones	No. of reversed resonance cones	Wave mode	Range of ω or ω_N	Fig.
O1	<1	$-$	0	0	0	0	Ord.	$\omega_N \leqslant \omega < \infty$	5.4
O2	>1	$+$	0	0	1	0	Ord.	$\omega_{S1} \leqslant \omega \leqslant \mathrm{Min}(\omega_N, \omega_H)$	5.5
							whistler		
O3	>1	$+$	1	0	1	0	Ord.		5.6
							whistler	$0 < \omega \leqslant \omega_{S1}$	
Cut-off	<0						Ord.	$\omega_H \leqslant \omega \leqslant \omega_N$	—
E1	<1	$+$	0	0	0	0	Ext.	$\omega_{C2} \leqslant \omega < \infty$	5.7
E2	>1	$-$	0	0	0	1	Ext. Z	$\omega_R \leqslant \omega \leqslant \omega_U$	5.8
E3	>1	$-$	0	1	0	1	Ext. Z	$\mathrm{Max}(\omega_N,\omega_H) \leqslant \omega \leqslant \omega_R$	5.9
E4	>1	$-$	1	1	0	0	Ext.	$\omega_{NS} \leqslant \omega_N \leqslant \omega \leqslant \omega_H$	5.10
E5	<1	$+$	1	0	0	0	Ext.		
							Z if $Y = 1$	$\omega_{S2} \leqslant \omega \leqslant \omega_N$	5.11
E6	<1	$+$	0	0	0	0	Ext.		
							Z if $Y < 1$	$\omega_{C1} \leqslant \omega \leqslant \omega_{S2}$	5.12
E7	>1	$-$	0	0	0	0	Ext.	$\omega_N \leqslant \omega_{NS}$ and $\omega < \omega_H$	5.13
Cut-off	<0						Ext.	$\omega_U \leqslant \omega \leqslant \omega_{C2}$	
Cut-off	<0						Ext.	$0 < \omega \leqslant \omega_{C1}$	

list and classify the various possible forms of the refractive index surface and the associated ray surface. There are now only two parameters, the electron concentration N_e now written simply as N, and ω/ω_H proportional to frequency, so it is possible to use a diagram in two dimensions. Clemmow and Mullaly (1955) used a diagram of Y vs X. In it lines of constant frequency were lines of constant Y, and lines of constant N were parabolae. Later authors have used Y^2 vs X so that lines of

Fig. 5.5. See caption of fig. 5.4. Region O2. Both refractive index surface and ray surface have two sheets and forward resonance cones and both are convex towards the origin. When $\omega_N < \omega_H$ and ω increases and approaches the value ω_N, the refractive index surface is two narrow cone-like surfaces closed at their inner ends and stretching to infinity. In the limit $X \to 1$ they shrink to two segments of the line $\Theta = 0$ beyond the window points $n = \pm\{Y/(Y-1)\}^{\frac{1}{2}}$. See §§5.2 (item (7)) and 4.11, 4.12. When $\omega_N > \omega_H$ and $\omega \to \omega_H$ the shape is similar but the closed inner ends of the tubes are beyond the window points and these points move to infinity in the limit $Y \to 1$. The curves marked T are for $\omega = \omega_{S1}$, and similar curves appear also in fig. 5.6. In this example $Y = 4$.

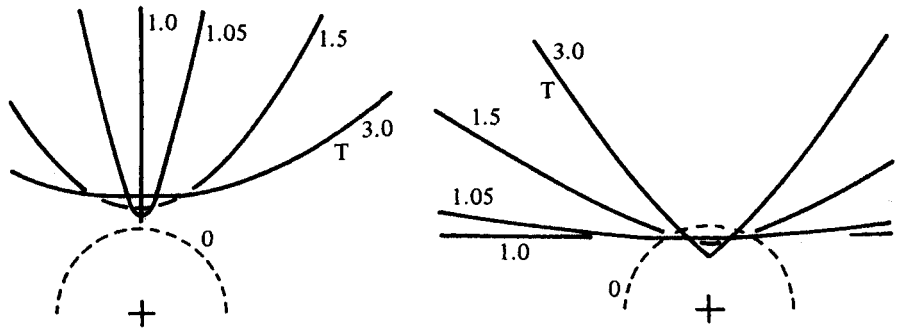

Fig. 5.6. See caption of fig. 5.4. Region O3. Both refractive index surface and ray surface have two sheets, forward resonance cones and forward Storey cones. This is the form for the simplest case of whistlers (Storey, 1953). The ray surface has an optic ray axis at $\beta = 0$; §§ 5.5. The curves marked T are for $\omega = \omega_{S1}$, and similar curves appear also in fig. 5.5. In this example $Y = 22$.

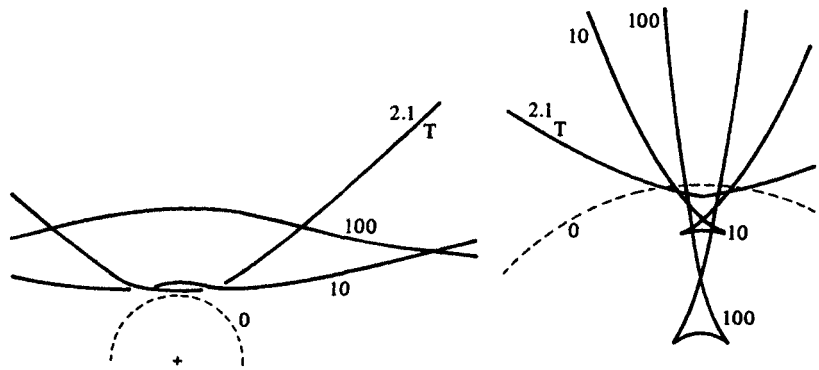

Fig. 5.7. See caption of fig. 5.4. Region E1. Both refractive index surface and ray surface are concave towards the origin. When ω is near to ω_{C2} the refractive index surface is a small ellipsoid (5.7) and the ray surface is a large ellipsoid (5.37). In the limit of cutoff $\omega \to \omega_{C2}$ the refractive index surface shrinks to a point and the ray surface expands to infinity; §§ 5.2, 5.4. In this example $Y = 0.5$.

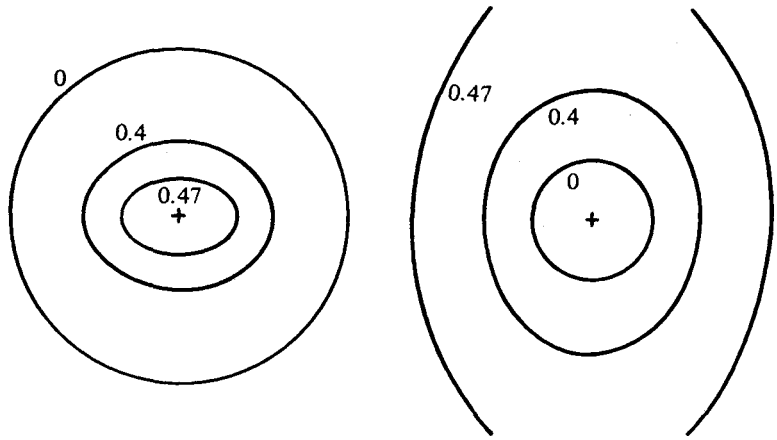

Fig. 5.8. See caption of fig. 5.4. Region E2. Both refractive index surface and ray surface have one sheet and are convex towards the origin. They have reversed resonance cones. This is one of the forms for the Z-mode. The curves marked T are for $\omega = \omega_R$ and the same curves appear in fig. 5.9. In this example $Y = 0.6$.

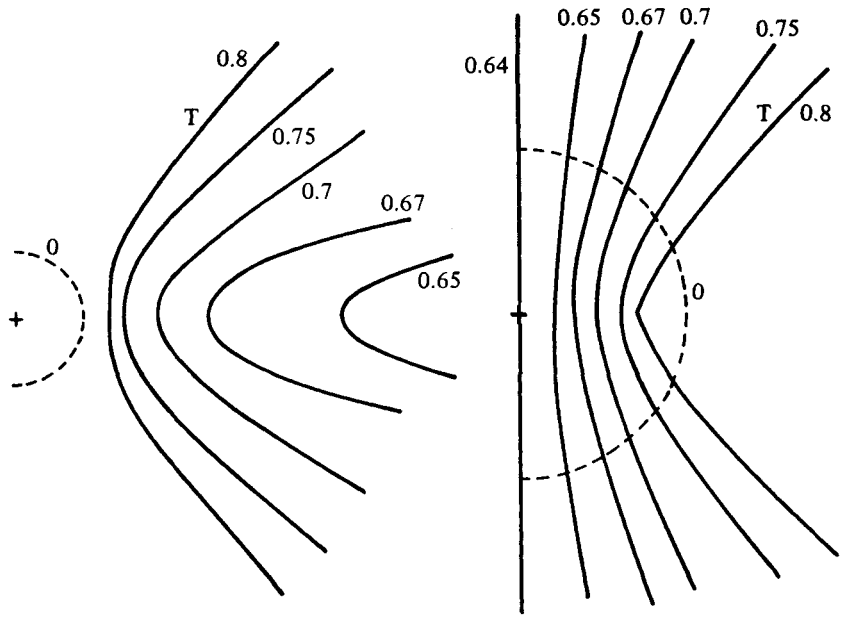

constant N are straight lines through the origin. In this book we use $1/Y$ vs $X^{\frac{1}{2}}/Y = \omega_N/\omega_H$ so that the ordinate is proportional to frequency and independent of N, and the abscissa is proportional to $N^{\frac{1}{2}}$ and independent of ω. Thus for all frequencies a vertical line refers to the same plasma.

In the Appleton–Lassen formula (4.48) or its equivalent forms (4.67), (4.68) (second expression), when collisions are neglected and X is real, the square root can never be zero or infinite for any frequency when $\sin\Theta \neq 0$. Thus the square root never reverses sign when ω or N changes. The positive value when used in (4.48) gives the refractive index n_O for the ordinary wave, as defined in § 4.15, and the negative value gives n_E for the extraordinary wave. The two values n_O, n_E are continuous distinct functions of ω and N for all real ω and N, except where one of them has a resonance. We therefore use separate classification diagrams for the ordinary and extraordinary waves. In the limit $\sin\Theta \to 0$, n_O and n_E can be equal at points in refractive index space called window points, §§ 4.11, 4.12, 5.2 Item (7), but only if

Fig. 5.9. See caption of fig. 5.4. Region E3. Both refractive index surface and ray surface have one sheet, reversed resonance curves and reversed Storey cones. This is another form for the Z-mode. If $\omega_N > \omega_H$ and $\omega \to \omega_N$, $X \to 1$, the limiting form of the refractive index surface is the unit sphere together with the two segments of the line $\Theta = 0$ beyond the points $n = \pm 1$. The limiting form of the ray surface is the sphere $V = c$ together with the two planes $V\cos\beta = \pm c$. If $\omega_N < \omega_H$ and $\omega \to \omega_H$ ($X < 1$, $Y \to 1$), the resonance cones of the ray surface move in towards $\Theta = 0, \pi$. If ω changes to a value less than ω_H the boundary is crossed into region E4 and the refractive index surface is then closed at $\Theta = 0, \pi$ as in fig. 5.10. The curves marked T are for $\omega = \omega_R$ and the same curves appear in fig. 5.8. In this example $Y = 0.6$.

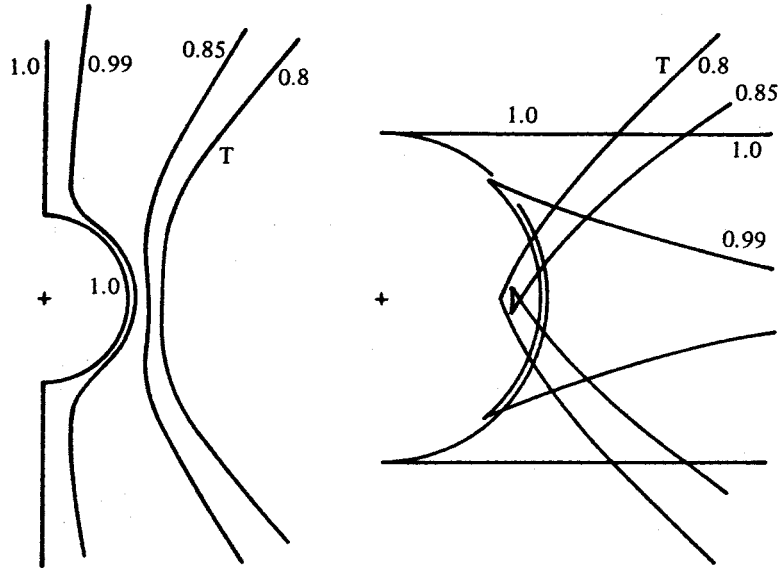

Fig. 5.10. See caption of fig. 5.4. Region E4. Both refractive index surface and ray surface are closed and have a Storey cone and a reversed Storey cone. When the boundary, marked $\omega_{RS1} - \omega_{RN} - \omega_{RS2}$ in fig. 5.3, is reached, these two cones move together as shown by the curves marked T which appear also in fig. 5.13. The cones disappear after the boundary is crossed. In the limit $\omega \to \omega_N$, $X \to 1$, the refractive index surface shrinks to the unit sphere together with the two segments of the line $\Theta = 0$ between $n = \pm 1$ and the window points $n = \pm\{Y/(Y-1)\}^{\frac{1}{2}}$. The limiting form of the ray surface is the sphere $V = c$ together with the two pairs of planes $V\cos\beta = \pm c\{(Y-1)/Y\}^{\frac{1}{2}}$ and $V\cos\beta = \pm c$. In this example $Y = 1.15$.

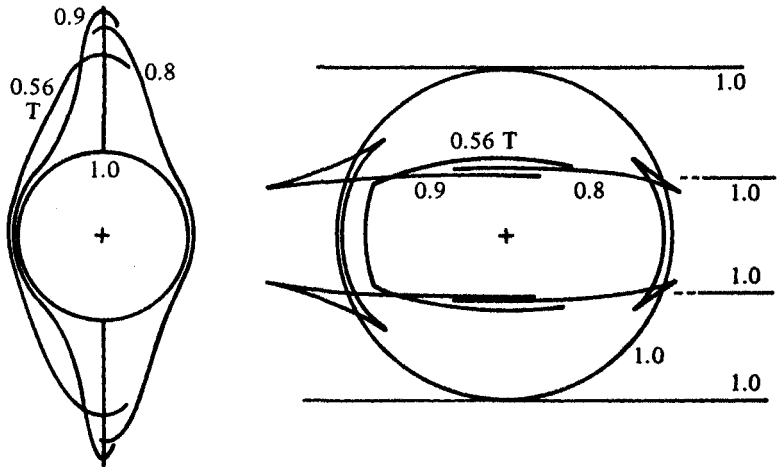

Fig. 5.11. See caption of fig. 5.4. Region E5. Both refractive index surface and ray surface are closed and have a Storey cone. The ray surface has an optic ray axis at $\beta = 0$; §§ 5.5. In the limit $\omega \to \omega_N$, $X \to 1$ the refractive index surface approaches the unit sphere together with the two segments of the line $\Theta = 0$ between the points $n = \pm 1$ and the window points $n = \pm\{Y/(Y+1)\}^{\frac{1}{2}}$. The limiting form of the ray surface is the sphere $V = c$ together with the two pairs of planes $V\cos\beta = \pm c$ and $V\cos\beta = \pm c\{(Y+1)/Y\}^{\frac{1}{2}}$. The curves marked T are for $\omega = \omega_{S2}$ and appear also in fig. 5.12. In this example $Y = 1.15$.

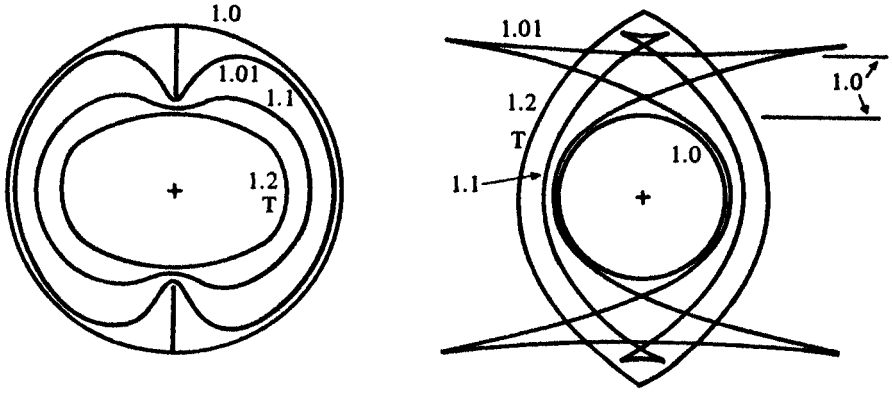

$X = 1$. It is therefore important to note the behaviour of the refractive index surfaces in the limit $X \to 1$ (see captions of figs. 5.4, 5.5, 5.9–5.11).

For the more general collisionless plasma, the square root in (4.51) or (4.68) (first expression) still can never be zero, when $\sin\Theta \cos\Theta \neq 0$, but it can be infinite. The situation is therefore a little more complicated but it turns out that n_O and n_E are still distinct functions for all frequencies for a given plasma.

Fig. 5.2 shows the classification diagram for the ordinary wave in a collisionless electron plasma. Throughout any one of the three regions marked O1, O2, O3, the

Fig. 5.12. See caption of fig. 5.4. Region E6. The topology is the same as for region E1, fig. 5.7. The curves marked T are for $\omega = \omega_{S2}$ and appear also in fig. 5.11. In this example $Y = 0.5$.

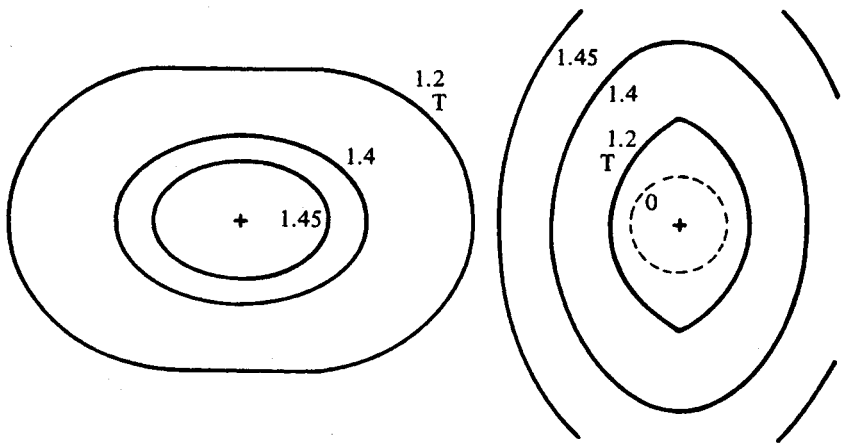

Fig. 5.13. See caption of fig. 5.4. Region E7. The topology is the same as for region O1, fig. 5.4, but the transition curve T is different. It is for the boundary marked $\omega_{RS1} - \omega_{RN} - \omega_{RS2}$ in fig. 5.3, and it appears also in fig. 5.10. In this example $Y = 1.15$.

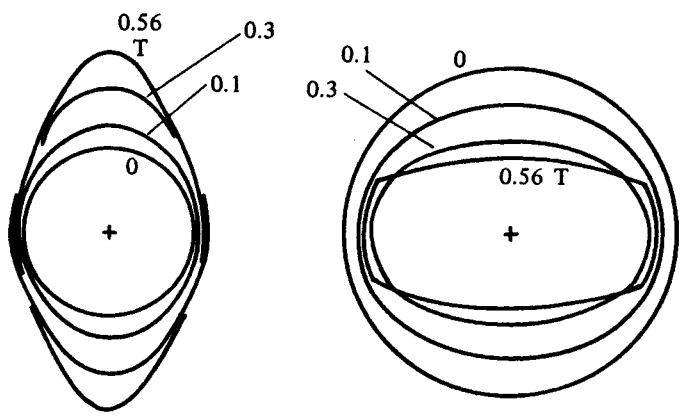

refractive index surface has the same form, figs. 5.4, 5.5, 5.6 respectively. There is one region, shaded and marked 'cut-off' where n_0^2 is negative for all Θ. Similarly fig. 5.3 shows the classification diagram for the extraordinary wave. There are now seven different forms of refractive index surface for regions E1 to E7 and shown in figs. 5.7–5.13 respectively, and there are two separate regions of 'cut-off'. The properties of the ten different forms are summarised in table 5.1.

The regions can be further subdivided depending on the behaviour of the group velocity. Details are not given in this book but see Booker (1975), Walker (1977b).

The boundary curves in figs. 5.2 and 5.3 show where a transition occurs from one type of refractive index and ray surface to another. Examples of the limiting form of these surfaces at a transition are shown in some of the figs. 5.4 to 5.13, and are marked with a T. The boundary curves are labelled with symbols giving the value of ω. Thus, in figs. 5.2, 5.3, ω_N is the plasma frequency and ω_H is the gyro-frequency. In fig. 5.2 the frequency ω_{S1} is where

$$\varepsilon_2 + \varepsilon_3 = 0, \quad X = 2(1 - Y)/(2 - Y) \tag{5.50}$$

(Walker, 1977b; compare (5.15)). When ω decreases through the value ω_{S1}, Storey cones appear at $\Theta = 0$ and π and move to greater values of Θ and $\pi - \Theta$ respectively (figs. 5.5, 5.6).

In fig. 5.3 the frequencies ω_{C1}, ω_{C2} are the cut-off frequencies where $X = 1 + Y$, $1 - Y$ respectively; (3.59), (3.60). The frequency ω_U is the upper hybrid resonance frequency where $X = 1 - Y^2$, (3.62). The frequency ω_{S2} is where (5.14) (5.15) are satisfied. When ω increases through the value ω_{S2}, Storey cones appear at $\Theta = 0$ and π and move to greater values of Θ and $\pi - \Theta$ respectively (figs. 5.12, 5.11). The frequency ω_R is where (5.18), (5.19) are satisfied. When ω decreases through the value ω_R reversed Storey cones appear at $\Theta = \frac{1}{2}\pi$ and move to greater values of $|\frac{1}{2}\pi - \Theta|$ (figs. 5.8, 5.9).

5.7. Dependence of refractive index on frequency

In ch. 4 examples were given, in figs. 4.3–4.6, to show how the two refractive indices of an electron plasma depend on the electron concentration N and the wave normal angle Θ, when the frequency is held constant. It is also of interest to give curves that show how the two values of n^2 depend on frequency for a plasma with a given fixed N. Examples are given for the two cases $\omega_N < \omega_H$, fig. 5.14 and $\omega_N > \omega_H$, fig. 5.15. These figures use the same conventions as in figs. 4.3, 4.5, 4.6. Thus curves for longitudinal propagation $\Theta = 0$ are shown as broken lines and curves for transverse propagation $\Theta = \frac{1}{2}\pi$ are shown as chain lines. The continuous lines are for an intermediate value of Θ. The marked frequencies in these two figures can be identified in the C.M.A. type diagrams, figs. 5.2, 5.3.

Some of the main features to be noted in these figures are as follows:

(1) For any wave normal angle Θ in the range $0 < \Theta < \frac{1}{2}\pi$, the curves of n^2 can never cross those for $\Theta = 0$ or $\Theta = \frac{1}{2}\pi$, except at the cut-off frequencies (proved in § 5.2 item (12)). Hence the curve for the ordinary wave always lies within the region shaded with dots and that for the extraordinary wave always lies in the region with line shading.

(2) The vertical line $\omega/\omega_N = 1$ ($X = 1$) is part of the curves when $\sin\Theta = 0$ (§§ 4.11, 4.12). In fig. 5.14, where $Y > 1$ when $X = 1$, the segment of this vertical line between the two real window points (P, P_2 in fig. 5.14) is for the extraordinary wave, and the remaining segments are for the ordinary wave. As the limit $|\sin\Theta| \to 0$ is approached, the curve for the extraordinary wave makes a steep traverse between regions close to the two window points. In fig. 5.15, where $Y < 1$ when $X = 1$, one of the two window points is where n^2 is negative. The segment of the line $\omega/\omega_N = 1$ between these window points is for the ordinary wave, and the remaining segments are for the extraordinary wave. As the limit $|\sin\Theta| \to 0$ is approached, the curve for the ordinary wave makes a steep traverse between regions close to the two window points; compare § 4.11.

Fig. 5.14. Curves showing how the square n^2 of the refractive index, for a cold electron magnetoplasma, depends on frequency when collisions are neglected, $U = 1$. The plasma frequency $\omega_N/2\pi$ and the electron gyro-frequency $\omega_H/2\pi$ are held constant and in this example $\omega_N/\omega_H = \frac{2}{3}$. The continuous curves are for $\Theta = 30°$. The broken curves are for longitudinal propagation $\sin\Theta = 0$, and the chain curves are for transverse propagation $\cos\Theta = 0$. For any other Θ the curves for the ordinary wave must lie within the regions shaded with dots, and those for the extraordinary wave within the regions shaded with lines. Compare figs. 4.3–4.6.

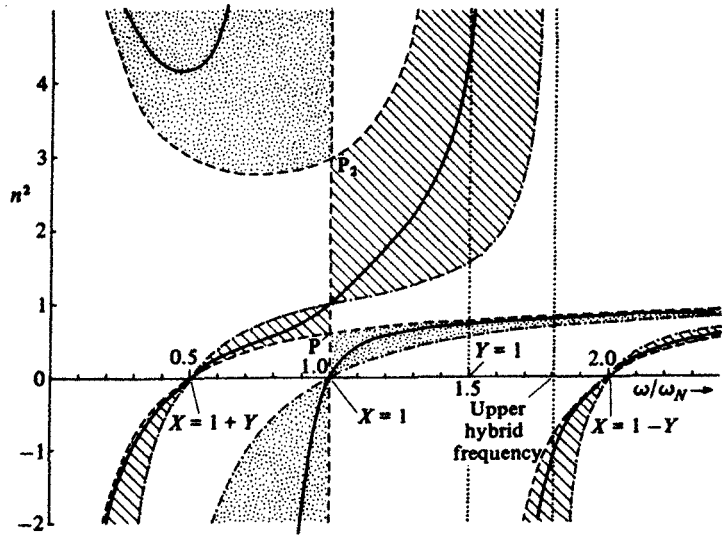

(3) The ordinary wave shows cut-off where $\omega/\omega_N = 1 (X = 1)$ for all Θ.

(4) The extraordinary wave shows cut-off where

$$\frac{\omega}{\omega_N} = \left\{\frac{1}{4}\left(\frac{\omega_H}{\omega_N}\right)^2 + 1\right\}^{\frac{1}{2}} \mp \frac{1}{2}\frac{\omega_H}{\omega_N} \tag{5.51}$$

for $X = 1 \pm Y$ respectively, for all Θ.

(5) Let ω_C denote any one of the cut-off frequencies mentioned in (3) and (4) above. Then the n^2 that is cut off is given by

$$n^2 = K(\omega - \omega_C) + O(\omega - \omega_C)^2 \tag{5.52}$$

where K is a positive constant (compare § 5.2 item (10)). When $X \approx 1 + Y$ it can be shown from (5.7) that

$$K = (2 + Y)/\{(1 + Y)(1 + \cos^2\Theta)\}. \tag{5.53}$$

When $X \approx 1 - Y$, (5.7) with the sign of Y reversed gives

$$K = (2 - Y)/\{(1 - Y)(1 + \cos^2\Theta)\}. \tag{5.54}$$

For positive X this can only occur where $Y < 1$. When $X \approx 1$, ε_3 is small and a formula analogous to (5.7) then gives $n^2 \approx \varepsilon_3 \operatorname{cosec}^2\Theta$. Hence for the cut-off at $X = 1$

$$K = 2\operatorname{cosec}^2\Theta \quad (\Theta \neq 0) \tag{5.55}$$

Thus the curve of n^2 versus ω always has a positive slope at cut-off. But n is proportional to $(\omega - \omega_C)^{\frac{1}{2}}$ so that near cut-off

$$\frac{dn}{d\omega} \approx \frac{K}{2n} \propto (\omega - \omega_C)^{-\frac{1}{2}}. \tag{5.56}$$

This tends to infinity as cut-off is approached.

Fig. 5.15. Similar to fig. 5.14 but $\omega_N/\omega_H = 1.5$ and the continuous curves are for $\Theta = 45°$. Note that the ordinate scale is different for the two parts of the figure.

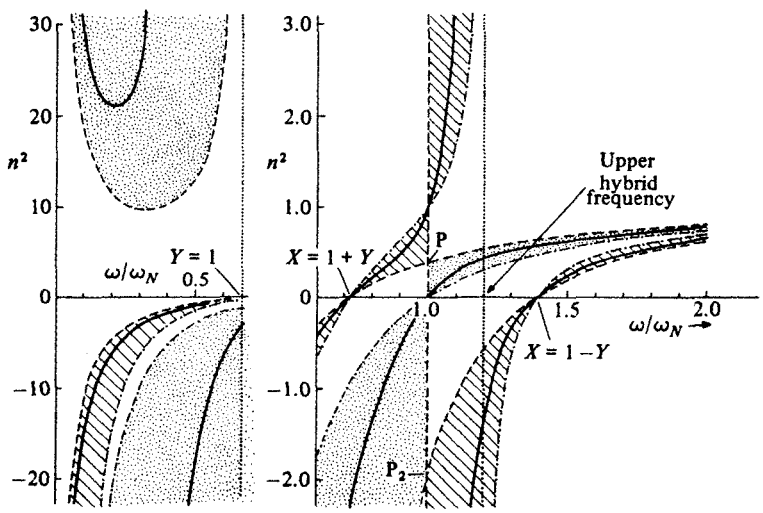

(6) The ordinary wave shows a resonance where

$$\left(\frac{\omega}{\omega_N}\right)^2 = \frac{1}{2} + \frac{1\omega_H^2}{2\omega_N^2} - \left\{\frac{1}{4}\left(\frac{\omega_H^2}{\omega_N^2} + 1\right)^2 - \frac{\omega_H^2}{\omega_N^2}\cos^2\Theta\right\}^{\frac{1}{2}} \tag{5.57}$$

which is derived from (4.76). When $\sin\Theta = 0$ this is where $\omega = \mathrm{Min}(\omega_H, \omega_N)$, that is ω_N in fig. 5.14, and ω_H in fig. 5.15. When $\cos\Theta \to 0$ this resonance occurs where $\omega/\omega_N \to 0$. For intermediate Θ this resonance is between these limits. It occurs in the branch of the curves for the whistler mode, and the refractive index surfaces are shown in fig. 5.6. In the limit $X \to \infty$, that is $\omega \to 0$, these surfaces extend round towards $\Theta \to \pm\frac{1}{2}\pi$.

(7) The extraordinary wave shows a resonance given by (5.57) when the first $-$ sign is changed to $+$. When $\sin\Theta = 0$ this is where $\omega = \mathrm{Max}(\omega_H, \omega_N)$ that is ω_H in fig. 5.14 and ω_N in fig. 5.15. When $\cos\Theta \to 0$ this resonance occurs at the upper hybrid resonance frequency (3.62), that is

$$\omega \to \omega_U = (\omega_N^2 + \omega_H^2)^{\frac{1}{2}}. \tag{5.58}$$

For intermediate Θ the resonance is between these limits. It occurs in the branch of the curves for the Z-mode, and the refractive index surfaces are shown in figs. 5.8, 5.9.

(8) Let ω_∞ denote either of the resonance frequencies mentioned in (6) and (7) above. Then it can be shown, from (4.76) or (4.77) that near a resonance, $n^2(\omega)$ has a simple pole so that it can be expressed as a Laurent series

$$n^2 = \frac{\mathscr{A}}{\omega - \omega_\infty}\{1 + O(\omega - \omega_\infty)\}. \tag{5.59}$$

It can further be shown that for the collisionless electron plasma

$$\mathscr{A} = \frac{-X(1 - Y^2\cos^2\Theta)^2(1 + Y^2\cos^2\Theta)\omega_\infty}{2\sin^2\Theta\{(1 - X\cos^2\Theta)^2 + X^2\cos^2\Theta\sin^{-2}\Theta\}}. \tag{5.60}$$

Thus when X and ω_∞ are positive, $\mathscr{A}$ is negative, so that n^2 is positive for frequencies slightly less than any ω_∞, or equivalently for values of X slightly greater than the value X_∞ at exact resonance. The property (5.59) also shows that, near resonance

$$\frac{\mathrm{d}n}{\mathrm{d}\omega} \approx -\frac{\mathscr{A}}{2n(\omega - \omega_\infty)^2} \propto (\omega - \omega_\infty)^{-\frac{3}{2}}. \tag{5.61}$$

This tends to infinity as resonance is approached. (Compare the property (5.56) at cut-off).

(9) The two values of n^2 are continuous and bounded functions of ω near $\omega = \omega_H$, that is $Y = 1$, except when $\sin\Theta = 0$.

(10) Both values of n^2 tend to infinity when $\omega \to 0$. It must, however, be remembered that the effect of ions has here been neglected. At low frequencies the ions have an important effect and introduce additional resonances and cut-offs. For an

actual plasma, at frequencies less than the smallest ion gyro-frequency, it can be shown that, when $\omega \to 0$, the two squared refractive indices tend to the bounded values $n^2 = \varepsilon_1$, $\varepsilon_1 \sec^2\Theta$ where ε_1 is given by the first two terms of (3.72).

When collisions are allowed for $n = \mu - i\chi$ is complex and it would be necessary to draw curves of μ and χ versus ω. These would be similar in many of their properties to the curves of μ and χ versus X discussed in §4.16, figs. 4.7–4.11. In particular segments of the vertical line $\omega = \omega_N$ in figs. 5.14, 5.15 would not now form part of the curves when $\sin\Theta = 0$. As Θ increases and passes through the value Θ_t given by (4.96) the curves of $\mu(\omega)$ and $\chi(\omega)$, near $\omega = \omega_N$, would show intersections or bends similar to those in figs. 4.7–4.11. The curves would join exactly when $\Theta = \Theta_t$, as in fig. 4.9. When $\Theta > \Theta_t$, the curves of $\mu(\omega)$ and $\chi(\omega)$ for the ordinary wave would be continuous for all ω, and similarly for the extraordinary wave. When $\Theta < \Theta_t$ the two curves would still be continuous for all ω including $\omega = \omega_N$. But one curve would be ordinary for $\omega < \omega_N$ and extraordinary for $\omega > \omega_N$, and conversely for the other curve. This is just the same change of description as was needed in §4.16 near $X = 1$.

5.8. Group velocity

In radar and in many radio experiments (see § 1.6), pulses of radio waves are used. A pulse of this kind can be thought of as the signal from a transmitter that generates a constant frequency ω_1 and that is switched on for a short time T. The study of the propagation of pulses is useful for introducing the concept of group velocity, but the importance of this concept is not confined to the study of pulses.

A pulsed radio signal can be represented by a Fourier integral thus

$$F(t) = \int_{-\infty}^{\infty} M(\omega) e^{i\omega t}\, d\omega \tag{5.62}$$

where F is some field component in the radio wave. The form of the function $M(\omega)$ depends on the shape of the pulse which is usually a signal of constant frequency ω_1 and roughly constant amplitude lasting for a time T, which, though short, is long compared with $1/\omega_1$. T may be 200 μs or less and $\omega_1/2\pi$ may be anything from 50 kHz upwards. $M(\omega)$ then has maxima at or near $\omega = \pm\omega_1$, and ω_1 is therefore called the predominant frequency. If $T \gg 1/\omega_1$, the maxima are narrow so that only frequencies very close to $\pm\omega_1$ play a part in the propagation of the pulse. Because $F(t)$ is real it follows that $|M(\omega)|$ is symmetric and $\arg M(\omega)$ is antisymmetric about $\omega = 0$. The centre of the pulse is assumed to be at $t = 0$ which ensures that $\arg M(\omega)$ does not vary appreciably in a small range near ω_1. In this chapter the exact form of $M(\omega)$ is unimportant. It is considered in more detail in §11.16.

Suppose now that the signal (5.62) is the field of an infinite plane wave with its wave normal in the z direction, and let it be launched where $z = 0$ into a

homogeneous plasma. Then each component frequency gives a wave whose field contains the factor $\exp(-ikn z)$ as in (2.32), and the field at a distance z from the launching point is

$$F(t, z) = \int_{-\infty}^{\infty} M(\omega) \exp\{i(\omega t - \omega n z/c)\} d\omega. \tag{5.63}$$

This integral is the sum of contributions from frequencies in narrow ranges near $\pm \omega_1$. When these contributions have the same phase, the integral has its greatest value. Thus the pulse reaches the distance z at a time t when the phase of the exponential term in (5.63) is stationary with respect to changes of ω. This gives

$$t - \frac{\partial(\omega n) z}{\partial \omega} \frac{1}{c} = 0 \text{ for } \omega = \omega_1 \tag{5.64}$$

so that the velocity $\mathscr{U}_z = z/t$ of the pulse in the z direction is given by

$$c/\mathscr{U}_z = n'(\omega_1) = \partial(\omega n)/\partial\omega \quad (\omega = \omega_1). \tag{5.65}$$

If the velocity of the pulse has any component perpendicular to the z direction, this could not be detected in the present example since the pulse was assumed to be an infinite plane wave. To study the x and y components of the velocity it would be necessary to consider a pulse of limited extent in the x and y directions, that is a 'wave packet' and this is done later in this section. It is shown that for an isotropic medium the wave packet travels in the direction of the wave normal, that is the z direction, so that $\mathscr{U}_z$ is the true velocity of the pulse. But for an anisotropic medium the pulse travels in the direction of the ray, that is at an angle α to the z axis as shown in § 5.3, and given by (5.33).

The true velocity $\mathscr{U}$ of a wave packet is called the 'group velocity'. Thus for an isotropic medium (5.65) gives the value $\mathscr{U}_z = \mathscr{U}$ of the group velocity. For a collisionless isotropic electron plasma, (4.10) gives

$$n = (1 - \omega_N^2/\omega^2)^{\frac{1}{2}}, \quad n' = \partial(\omega n)/\partial\omega = (1 - \omega_N^2/\omega^2)^{-\frac{1}{2}} = 1/n. \tag{5.66}$$

In this case $\mathscr{U} = c/n'$ from (5.65), and the phase velocity $v = c/n$ is the same as the ray velocity V, (5.34), (5.35) so that

$$\mathscr{U} V = c^2. \tag{5.67}$$

It is interesting that several other types of wave motion obey a relation similar to (5.67). For example, it is true for one mode in a loss-free wave guide. In wave mechanics, for the waves associated with particles of zero potential energy but various total energies, when treated relativistically, it can be shown that the group velocity $\mathscr{U}$ is the velocity of the particle, and (5.67) is true when V is the phase velocity. But for waves in a plasma it is not true except in the special case (5.66).

For a general anisotropic plasma it was shown in § 5.3 that for a plane wave the direction of energy propagation is the direction of the ray and makes an angle α with

the wave normal, (5.33). It is shown below that the velocity $\mathscr{U}$ of a wave packet, that is the group velocity, is in the direction of the ray, so that $\mathscr{U}_z = \mathscr{U}\cos\alpha$ is its component in the direction of the wave normal. Thus from (5.65)

$$\mathscr{U} = c/(n'\cos\alpha). \tag{5.68}$$

It must be emphasised that in general the group velocity is not equal to c/n'.

To find the velocity of a wave packet consider again the expression (5.29) for the field F emitted from a source at the origin. It represents the field as an angular spectrum of plane waves and was derived by expressing it as a Fourier integral in space. We now suppose that the emitted signal is a pulse, like (5.62) so that the amplitude A in (5.29) is also a function of the frequency ω, and the integral is a triple integral. In (5.29) the two variables of integration are n_ξ, n_η and they determine the direction of the wave normal of the wave represented by the integrand, but any two combinations of n_ξ, n_η, n_ζ could have been used. We now have to choose three combinations of the four variables $\omega, n_\xi, n_\eta, n_\zeta$ to determine the direction of the wave normal and the frequency. It is convenient to use the three components of the wave vector

$$\boldsymbol{\kappa} = (\kappa_\xi, \kappa_\eta, \kappa_\zeta) = \frac{\omega}{c}(n_\xi, n_\eta, n_\zeta) \tag{5.69}$$

(compare (2.31). In many branches of physics $\boldsymbol{k}$ is used instead of $\boldsymbol{\kappa}$). Then the field of the signal is

$$F(t, \xi, \eta, \zeta) = \int_{-\infty}^{\infty}\int_{-\infty}^{\infty}\int_{-\infty}^{\infty} A(\omega, \boldsymbol{\kappa})\exp\{\mathrm{i}(\omega t - \xi\kappa_\xi - \eta\kappa_\eta - \zeta\kappa_\zeta)\}\,\mathrm{d}\kappa_\xi\mathrm{d}\kappa_\eta\mathrm{d}\kappa_\zeta. \tag{5.70}$$

Now it is assumed that the signal is a pulse as in (5.62) so that A is appreciable only near $\omega = \pm\omega_1$ where ω_1 is the predominant frequency. It is further assumed that the signal is in a narrow beam so that the wave vectors κ are all near a predominant value $\boldsymbol{\kappa}_1$. Thus A is appreciable only near $\boldsymbol{\kappa} = \pm\boldsymbol{\kappa}_1$. The signal is therefore a wave packet, that is a pulse travelling along the beam which is its path. We now invoke again the principle of stationary phase which was used to derive (5.31) and (5.64). The signal F in (5.70) is appreciable only for those values of t, ξ, η, ζ for which the phase, that is the exponent of the integrand, is stationary for small changes of κ_ξ, κ_η, κ_ζ, when $\omega = \omega_1$ and $\boldsymbol{\kappa} = \boldsymbol{\kappa}_1$. This gives

$$\xi/t = \partial\omega/\partial\kappa_\xi, \quad \eta/t = \partial\omega/\partial\kappa_\eta, \quad \zeta/t = \partial\omega/\partial\kappa_\zeta \quad (\omega = \omega_1, \boldsymbol{\kappa} = \boldsymbol{\kappa}_1). \tag{5.71}$$

These are just the three components of the velocity of the wave packet, that is of the group velocity $\mathscr{U}$. The result (5.71) is usually written in the shorthand notation

$$\mathscr{U} = \partial\omega/\partial\boldsymbol{\kappa}. \tag{5.72}$$

It is well known and used in many branches of physics.

To use (5.72) it is necessary to express ω as a function of $\boldsymbol{\kappa} = \omega_1\boldsymbol{n}/c$. The equation

$\omega(\boldsymbol{\kappa}) = \omega_1$ is an equation relating $(\omega/c)(n_\xi, n_\eta, n_\zeta)$. It is just the equation of the refractive index surface. On this surface $\delta\omega$ must be zero so that

$$\frac{\partial\omega}{\partial\boldsymbol{\kappa}}\cdot\delta\boldsymbol{n} = \mathscr{U}\cdot\delta\boldsymbol{n} = 0. \tag{5.73}$$

But any allowed $\delta\boldsymbol{n}$ lies in the refractive index surface. Thus $\mathscr{U}$ is normal to this surface and therefore has the same direction as the ray.

For a plasma it is algebraically complicated to express ω as a function of $\boldsymbol{\kappa}$ or equivalently of $\boldsymbol{n}$. The dispersion relation (4.65) for an electron plasma is of sixth degree in ω and when ions are allowed for it is of still higher degree, and it would be necessary to solve this equation. It is much easier to use the result (5.68), which is studied in the following section. It can be shown (see problem 5.6) that the results (5.68) and (5.72) are the same.

5.9. Properties of the group velocity

In this section we study the dependence of group velocity, in an electron plasma, on electron concentration and on frequency. The dispersion relation (4.65) with (4.66) is used. The A used in these equations has no connection with the A used in § 5.8. Differentiation of (4.65) with respect to ω gives

$$4n(n^2A - B)\partial n/\partial\omega + n^4\partial A/\partial\omega - 2n^2\partial B/\partial\omega + \partial C/\partial\omega = 0. \tag{5.74}$$

Hence from (5.65)

$$n' = n + \omega\partial n/\partial\omega = \frac{n^4\left(A - \frac{1}{4}\omega\frac{\partial A}{\partial\omega}\right) - n^2\left(B - \frac{1}{2}\omega\frac{\partial B}{\partial\omega}\right) - \frac{1}{4}\omega\frac{\partial C}{\partial\omega}}{n(n^2A - B)}. \tag{5.75}$$

This is the group refractive index and is equal to $c/\mathscr{U}_z$ where $\mathscr{U}_z$ is the component of the group velocity in the direction of the wave normal. It is important in the theory of the probing of a horizontally stratified ionosphere by vertically incident pulses of radio waves. When a vertically incident wave packet enters the ionosphere it is deviated laterally (see § 10.12 and fig. 10.11) but the wave normal remains vertical. It travels up to a reflection level and returns by the same path. To find its travel time it is necessary to know only the vertical component $\mathscr{U}_z = c/n'$ of its velocity. This was at one time called the group velocity and some authors still use this term. The true group velocity is $\mathscr{U} = \mathscr{U}_z \sec\alpha$. Curves of n' versus X and tables have been published (Shinn and Whale, 1952; Shinn, 1955). Curves of group velocity versus frequency for both cold and warm plasmas were given by Aubry, Bitoun and Graff (1970).

When collisions are neglected, (4.66) shows that

$$\begin{aligned} A - \tfrac{1}{4}\omega\partial A/\partial\omega &= 1 - \tfrac{3}{2}X - Y^2(\tfrac{3}{2} - 2X) - 2XY^2\sin^2\Theta \\ B - \tfrac{1}{2}\omega\partial B/\partial\omega &= (1 - X)(1 - 3X) - Y^2(2 - 3X) - \tfrac{3}{2}XY^2\sin^2\Theta \\ -\tfrac{1}{4}\omega\partial C/\partial\omega &= -\tfrac{3}{2}X(1 - X)^2 - Y^2(\tfrac{1}{2} - X). \end{aligned} \tag{5.76}$$

These were used in (5.75) to calculate the curves of figs. 5.16, 5.17. They show examples of how n' depends on X and are for the same conditions as figs. 4.3, 4.6 respectively for n^2 vs X.

Equations (5.56) and (5.61) show that $\partial n/\partial\omega$ and therefore n' is infinite when either cut-off or resonance is approached and this can be seen in fig. 5.16, 5.17. It is important to know how n' approaches infinity in these two cases. In (5.75) near any cut-off condition all terms except n in the denominator are analytic functions of X.

Fig. 5.16. Shows how the group refractive index depends on X for a cold collisionless electron plasma. In this example $Y=\frac{1}{2}$. The continuous curves are for $\Theta = 23.27°$. The broken curves are for longitudinal propagation, $\sin\Theta = 0$. The broken curve for the extraordinary wave when $X < 0.5$ is extremely close to the continuous curve E and therefore is not shown. The chain curves are for transverse propagation $\cos\Theta = 0$. Note the change of name from O ordinary, to E extraordinary, where the broken curve crosses the line $X = 1$.

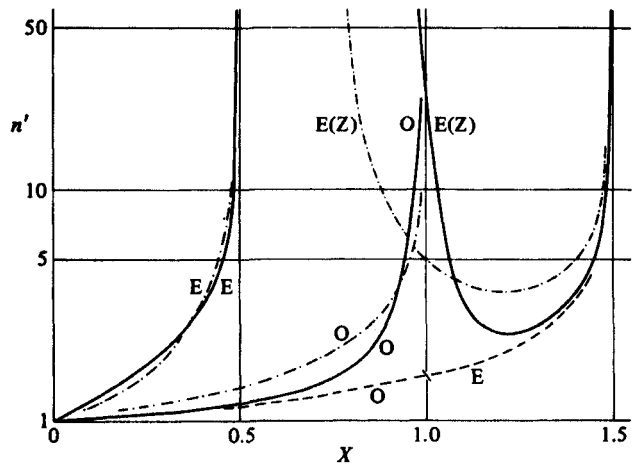

Fig. 5.17. Similar to fig. 5.16, but in this example $Y=2$.

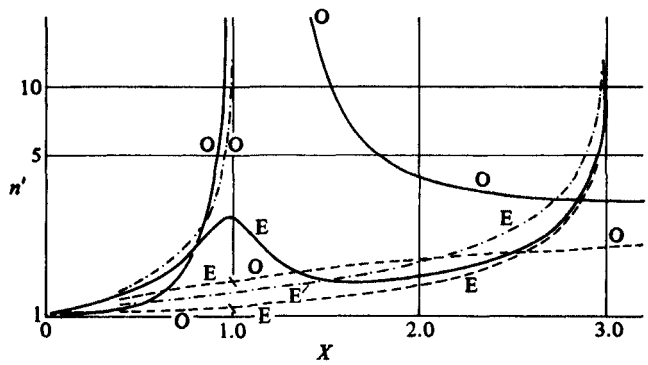

In them we may therefore give X its value at cut-off and set $n^2 = 0$, to give

$$n' \approx \tfrac{1}{4}\omega \frac{\partial C}{\partial \omega}/Bn. \tag{5.77}$$

For the ordinary wave near cut-off at $X = 1$, this gives $n' = \operatorname{cosec}^2\Theta/n$. Now (4.65) (4.66), with $U = 1$, show that $n^2 \approx (1 - X)\operatorname{cosec}^2\Theta$. Hence

$$n' \approx \operatorname{cosec}\Theta(1 - X)^{-\frac{1}{2}}. \tag{5.78}$$

Similarly for the extraordinary wave cut-off at $X = 1 + Y$, (5.77) gives $n' = (1 + \frac{1}{2}Y)/\{(1 + Y)(1 - \frac{1}{2}\sin^2\Theta)n\}$, and n^2 is given by (5.7). Hence

$$n' \approx (1 + \tfrac{1}{2}Y)\{(1 + Y)(1 + Y - X)\}^{-\frac{1}{2}}. \tag{5.79}$$

For the cut-off at $X = 1 - Y$ the result is (5.79) with the sign of Y reversed. In (5.78) and (5.79) it is the power $-\frac{1}{2}$ that is important and it is mentioned again in § 19.6.

The results (5.78), (5.79) show that for every real cut-off condition, n' is real when X is slightly less than its value at exact cut-off. This behaviour can be seen in figs. 5.16, 5.17. The same property holds for the refractive index n; § 5.2 item (10), § 5.7 item (5).

For a resonance a similar argument can be used. It is more complicated because A is zero at a resonance. But it can be shown from (5.75) after a little algebra, that near resonance

$$n' \approx -\tfrac{1}{4}\omega \frac{\partial A}{\partial \omega} n^3/B. \tag{5.80}$$

Now (4.65) (4.66), with $U = 1$, show that

$$n^2 \approx 2B/A = 2B(Y^2\cos^2\Theta - 1)^{-1}(X - X_\infty)^{-1} \tag{5.81}$$

where X_∞ is the value of X at resonance. Hence finally

$$\begin{aligned} n' \approx\ & Y|\sin\Theta|\{\sin^2\Theta + \cos^2\Theta(1 - Y^2)\} \\ & \times (1 + Y^2\cos^2\Theta)^{\frac{1}{2}}|1 - Y^2\cos^2\Theta|^{-3}X_\infty^{\frac{1}{2}}(X - X_\infty)^{-\frac{3}{2}} \end{aligned} \tag{5.82}$$

Here it is the factor $(X - X_\infty)^{-\frac{3}{2}}$ that is important. See § 19.6.

For every real resonance, (5.82) shows that n' is real when X slightly exceeds its value X_∞ at exact resonance. This behaviour can be seen in figs. 5.16, 5.17. The same property holds for the refractive index n; § 5.7 item (8).

To find the true group velocity $\mathscr{U} = c/n'\cos\alpha$ it is necessary to know the angle α. It can be found by differentiating (4.65) with respect to Θ, and is given, from (5.33), by

$$\tan\alpha = \frac{1}{n}\frac{\partial n}{\partial \Theta} = \frac{XY^2\sin\Theta\cos\Theta(n^2 - 1)}{2(An^2 - B)}. \tag{5.83}$$

Figs. 5.18–5.20 show an example of how $n'\cos\alpha = c/\mathscr{U}$ and α depend on frequency ω for a fixed value of the ray direction β. The advantage of plotting $c/\mathscr{U}$ versus frequency is that it is proportional to the time of travel of a pulsed signal over a fixed range in the given direction β. If the scale of $c/\mathscr{U}$ were linear, the curves would be the same shape as the record that would be obtained from an 'on-line' spectral analyser

of the type commonly used for studying whistlers (§ 13.8), when the source is an impulse. In figs. 5.18, 5.20, however, the scale of $c/\mathscr{U}$ is logarithmic. It should also be remembered that these results are for a homogeneous plasma and differ in some respects from observations made for an inhomogeneous plasma such as the ionosphere or the magnetosphere. On the path of a whistler the angle β is not constant.

The importance of the angle α may be illustrated by considering two space vehicles immersed in the homogeneous plasma. A radio signal is to be sent from one to the other by a directed radio beam. Suppose that the transmitting aerial has a large aperture which is energised with constant phase. If it were in free space this aerial would radiate a single narrow beam in the direction of its axis, normal to the aperture. When it is in the plasma the wave normal of the beam is still parallel to the aerial's axis, but there are two rays, ordinary and extraordinary, which leave the aerial in different directions, because they have different values of the angle α. If one of these rays is to reach the second vehicle, whose true direction makes an angle β with the earth's magnetic field, the aerial would have to be pointed in a direction that makes an angle $\Theta = \beta + \alpha$ with this magnetic field. Now α is itself a function of Θ. Thus when the aerial axis is rotated uniformly in a plane parallel to the magnetic field, the two beams do not rotate uniformly with it. There are cases where the ray direction $\Theta - \alpha$ decreases when Θ is increasing, for a small range of Θ, and it is then possible to find as many as four different directions of the transmitting aerial that will send a signal towards the second vehicle, with different times of travel. Examples

Fig. 5.18. Shows how $n' \cos\alpha = c/\mathscr{U}$ depends on frequency for a cold collisionless electron plasma, when the direction of the ray is fixed. In this example $\omega_N/\omega_H = \frac{2}{3}$ and the ray direction is $\beta = 10°$. The symbols by the curves indicate the regions of the CMA type diagrams, figs. 5.2, 5.3. Different abscissa scales are used in different parts of the range, to show up the details. The transition frequencies indicated by arrows are defined in §§5.6, 5.7. The point marked SC is where a Storey cone crosses the ray direction. Similarly RSC is where a reversed Storey cone crosses the ray direction. Note the change from ordinary to extraordinary at the two window points P, P_2 on the line $X = 1$,

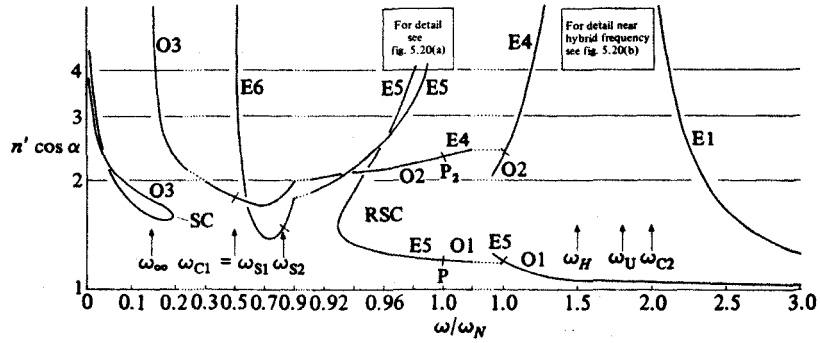

can be seen in fig. 5.19. For part of the branches O3 there are three different real values of α, and for part of the branches E5 there are four different values.

Some of the main features to be noted in figs. 5.18–5.20 are the following. It is assumed that $|\Theta| < \frac{1}{2}\pi$.

(1) The symbols by the various sections of the curves show the regions of the C.M.A. type diagrams, figs. 5.2, 5.3 that are applicable. They can be used, with table 5.1 and figs. 5.4–5.13, to find the shape of the refractive index surface and ray surface for each section.

(2) Two cut-off frequencies ω_{C1} and ω_{C2} appear in fig. 5.19. These would be the same for any other β. The group velocity is real when ω is slightly greater than each ω_C, and tends to ∞ when $\omega \to \omega_C$; see especially (5.80). In this limit $\tan\Theta = 2\tan\beta$ (see (5.37)) and $\alpha = \Theta - \beta$ so that, with $\beta = 10°$ in this example, $\alpha \to 9.42°$.

(3) In figs. 5.18, 5.19 there is one resonance frequency ω_∞ in the branch O3. This is where the frequency dependent resonance cone angle β_R is equal to the ray direction β. Thus the value of ω_∞ depends on β. This resonance is a forward resonance and the limiting value of α is $-90°$ (fig. 5.19), so that $\cos\alpha \to 0$. It was shown in § 5.9, equation (5.82) that at resonance $n' \to \infty$. It can also be shown (Budden and Stott, 1980, § 4.3) that $n'\cos\alpha \to \infty$, as in fig. 5.18. In fig. 5.20(b) there is another ω_∞ for the branch E2. This is a reversed resonance and $\alpha \to +90°$. Note that, for both these resonances $n'\cos\alpha$ is real when ω slightly *exceeds* ω_∞, whereas (5.82) shows that n' is real when $\omega < \omega_\infty$. It must be remembered that, when β is held constant, both Θ and α change when ω changes. The reader should satisfy himself that these changes will explain the behaviour of the curves near resonance.

(4) For the branch E4, $n'\cos\alpha \to \infty$ when $\omega \to \omega_H$ and in this limit $\alpha = -\beta$, so that $\Theta = 0$.

(5) The extreme left-hand curve O3 in figs. 5.18, 5.19 is for the whistler signal. The

Fig. 5.19. Shows how the angle α between the ray and the wave normal depends on frequency for the same example as in fig. 5.18. The wave normal direction is $\Theta = \beta + \alpha$ and here $\beta = 10°$.

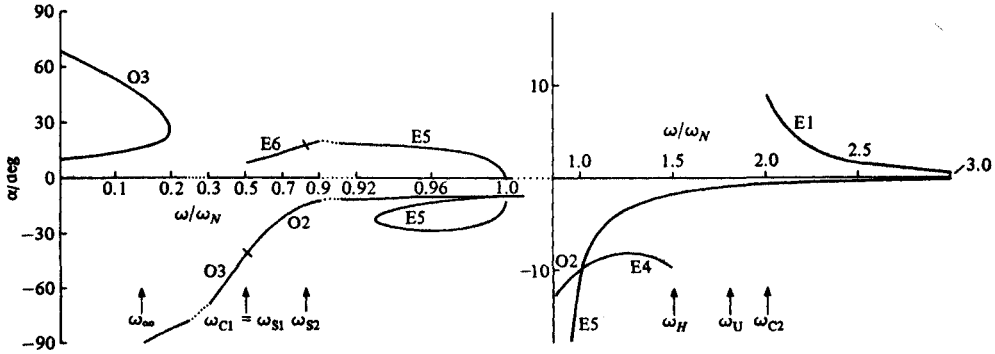

two branches of the curve can be identified in the ray surface, fig. 5.6(b). In the limit $\omega \to 0$ it can be shown (see problem 5.5) that $\tan\Theta = 2\tan\alpha$ whence it follows that in this example for $\beta = 10°$, the two limiting values of α are 10.7° and 69.3° as in fig. 5.19. But it should be remembered that at extremely low frequencies the form of the curves is very different when the effect of ions is allowed for; see Budden and Stott (1980). The frequency near $\omega/\omega_N = 0.17$ where $n'\cos\alpha$ is a minimum, corresponds to the 'nose frequency' of a whistler; see § 13.8.

(6) In fig. 5.18 there is a Storey cone, marked SC, in the whistler branch O3, and a reversed Storey cone, marked RSC, in the Z mode branch E5. In fig. 5.20(a) there is a reversed Storey cone, marked RSC, in the Z mode branch E4. These three cones can be identified in the ray surfaces, figs. 5.6(b), 5.11(b) and 5.10(b) respectively. These ray surfaces have cusps at values β_S of β which cross the actual ray direction β where the curves in figs. 5.18, 5.20 have a vertical tangent. Note that there are no cusps here for the group velocity $\mathscr{U}$ or its reciprocal.

(7) For frequencies very close to the electron plasma frequency (window frequency), two branches of the curves of $n'\cos\alpha$ tend to infinity as shown in fig. 5.20(a). They are associated with the part of the refractive index surface very close to the points $n = 1, \sin\Theta = 0$. This behaviour is interesting and needs further study. A start on this has been made by Budden and Stott (1980).

Another example of the dependence of $n'\cos\alpha = c/\mathscr{U}$ on frequency has been given

Fig. 5.20. Detail for fig. 5.18. Values of α in degrees are shown as numbers by the curves. (a) is for frequencies extremely close to the electron plasma frequency and is associated with the region of refractive index space very near to $n = 1, \Theta = 0$. (b) is for the Z-mode at frequencies extremely close to the upper hybrid resonance frequency ω_U.

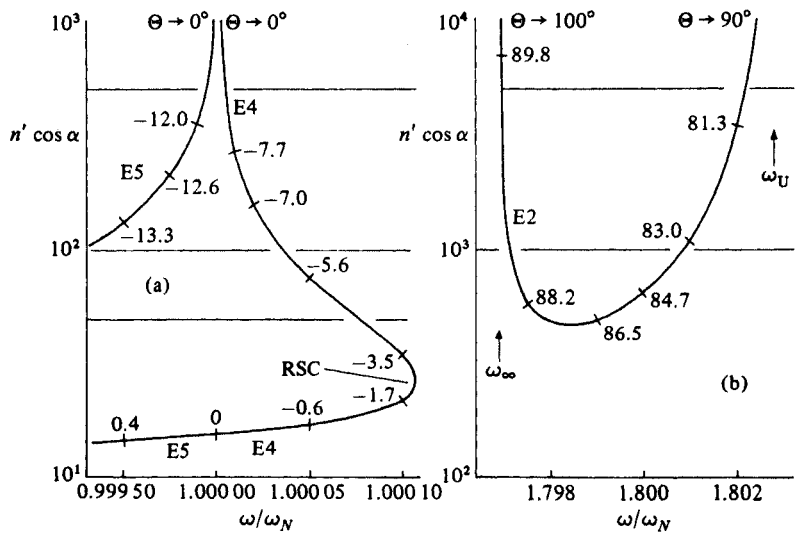

by Budden and Stott (1980) who allowed for the presence of ions. Curves of group velocity $\mathscr{U}$ versus ray direction β when the frequency is held constant have been given by Booker (1975, 1984), and Walker (1977a).

5.10. Effect of electron collisions on the group refractive index

The position of a wave packet at a given time was found in § 5.8 by expressing the condition that the phase must be stationary for small variations of frequency, and this led to the formula (5.65). If electron collisions are allowed for, the refractive index n is complex and its real part μ and imaginary part $-\chi$ are both frequency dependent. The dependence of χ on frequency leads to broadening and distortion of the wave packet; see, for example, Stratton (1941) ch. V; Gibbons and Rao (1957). But if the electron collision frequency ν is not too great, χ is small for a wave whose squared refractive index would be real and positive if collisions were neglected. Then the phase of the wave is determined mainly by μ, and if χ is neglected the travel time of a wave packet can be found exactly as in § 5.8. If u_z is the component of the wave packet's velocity in the direction of the wave normal, equation (5.65) is replaced by

$$c/u_z = \mu' = \mathrm{Re}(n') = \mu + \omega\frac{\partial\mu}{\partial\omega} = \mathrm{Re}\left(n + \omega\frac{\partial n}{\partial\omega}\right). \tag{5.84}$$

Here n' is now a complex number, and its real part μ' is often called the group refractive index. It is close to the real n' that would be obtained if collisions were

Fig. 5.21. Dependence on X of Re(n')–continuous curves, and Im(n')–broken curves, for an electron plasma at a fixed frequency. In this example $Y = 4$ and $\Theta = 23.27°$. The numbers by the curves are the values of Z. These curves are for the ordinary wave.

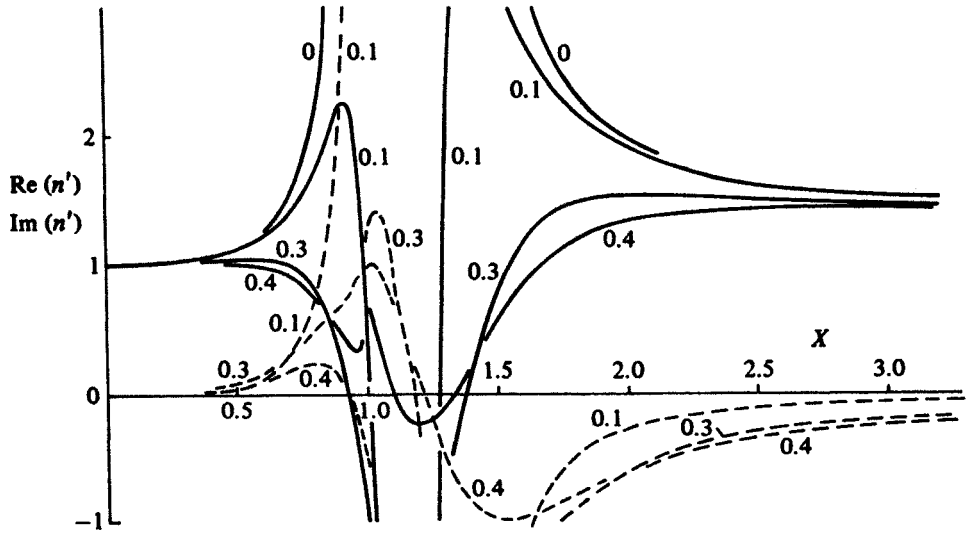

neglected, but the small difference can sometimes be important. For example in the vertical sounding of the ionosphere by radio pulses, the ionosonde technique § 1.7, it is sometimes necessary, when high accuracy is required, to allow for the effect of collisions on the group refractive index. This is especially true at lower frequencies because the effect depends on $Z = \nu/\omega$. It can be especially important at frequencies less than the electron gyro-frequency so that $Y > 1$.

To calculate μ' we first calculate n' and then take the real part. The formula (5.75) may still be used, where A and B are now complex numbers given by (4.66) and the complex n is given by (4.47). The factors (5.76) now have additional terms containing Z, as follows

$$\left.\begin{aligned} A - \tfrac{1}{4}\omega\partial A/\partial\omega &= 1 - \tfrac{3}{2}X - Y^2(\tfrac{3}{2} - 2X) - 2XY^2\sin^2\Theta + \tfrac{1}{2}Z^2(4X - 9) \\ &\quad + \tfrac{1}{4}\mathrm{i}Z(14X + 7Y^2 + 7Z^2 - 15) \\ B - \tfrac{1}{2}\omega\partial B/\partial\omega &= (1 - X)(1 - 3X - 6Z^2) - Y^2(2 - 3X) - \tfrac{3}{2}XY^2\sin^2\Theta \\ &\quad + \tfrac{1}{2}\mathrm{i}Z(20X - 7X^2 + 5Y^2 + 5Z^2 - 9) \\ -\tfrac{1}{4}\omega\partial C/\partial\omega &= -\tfrac{3}{2}X(1 - X)^2 - Y^2(\tfrac{1}{2} - X) \\ &\quad - \tfrac{3}{2}Z^2 + 3XZ^2 + \tfrac{3}{4}\mathrm{i}Z(6X - 5X^2 + Y^2 + Z^2 - 1). \end{aligned}\right\} \quad (5.85)$$

Figs. 5.21, 5.22 show some typical results, for the ordinary and extraordinary waves respectively. For further examples see Millington (1938a), Titheridge (1961b). The curves show how the real and imaginary parts of n' depend on X for a fixed frequency, and various values of Z. In this example Z_t, (4.27), is 0.3398. Thus the values 0.1, 0.3 of Z are less than Z_t and the curves in each figure are continuous, although some of them make large deviations near $X = 1$. By contrast the value $Z = 0.4$ is greater than Z_t. The curves for the ordinary wave when $X < 1$, fig. 5.21, are continuous with those for the extraordinary wave when $X > 1$, fig. 5.22, and vice

Fig. 5.22. The same as fig. 5.21, but for the extraordinary wave. The curve of Re(n') for $Z = 0$ is extremely close to that for $Z = 0.1$, and therefore only a part of it can be shown.

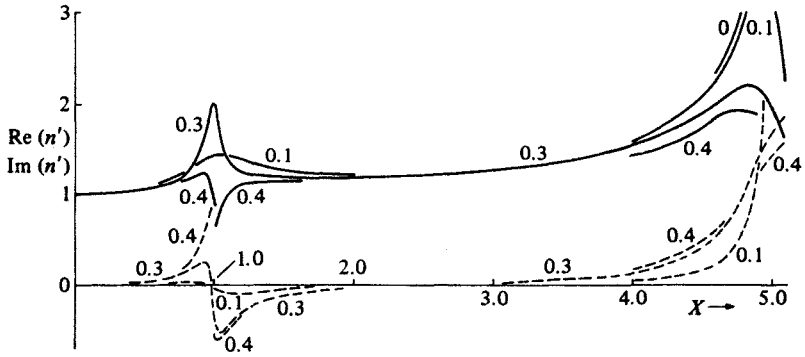

versa. This apparent discontinuity is simply the interchange of the names ordinary and extraordinary as described in §4.16.

When Z is equal to Z_t there is a coupling point on the real X axis at $X = 1$, as explained in §4.16. It can be shown that here both $\mathrm{Re}(n')$ and $\mathrm{Im}(n')$ are infinite. The proof is left to the reader (show that the denominator of (5.75) is zero).

PROBLEMS 5

5.1. The polar curves $n(\Theta)$ and $V(\beta)$ are the cross sections, by a plane through the axis, of a refractive index surface and its associated ray surface for a collisionless plasma. The angle between corresponding radii for the two curves is $\alpha = \Theta - \beta$. A Storey cone in either diagram may be defined as the cone $\Theta = \Theta_s$ or $\beta = \beta_s$ where $\partial\beta/\partial\Theta = 0$. Show that on a Storey cone $n\partial^2 n/\partial\Theta^2 - 2(\partial n/\partial\Theta)^2 - n^2 = 0$, and that this is the condition for a point of inflection of the refractive index surface. Show also that $\partial(1/V)/\partial\beta = n\sin\alpha/c$. Since this is bounded, the ray surface has a cusp at the Storey cone. If $\mathscr{U}$ is the group velocity show that $\partial\mathscr{U}/\partial\beta$ is infinite at a Storey cone. Hence show that a polar plot of $\mathscr{U}$ versus β does not have a cusp but a loop, at a Storey cone. (For examples see Walker, 1977a; Booker, 1975, 1984).

5.2. For the polar curves of problem 5.1 show that, at corresponding points, the product of the curvatures is $\cos^3\alpha/c$. Hence show that for $\Theta = \beta = 0$ in an electron plasma, the ray surface can have zero curvature only in the three conditions (a) $X = 1$ (What is then the value of V? See figs. 5.4, 5.5, 5.9, 5.10), (b) cut-off $X = 1 \pm Y$ (trivial because $V \to \infty$), and (c) $Y = 1$ (trivial because $V \to 0$). Show also that for $\Theta = \beta = \frac{1}{2}\pi$ the ray surface for the ordinary wave never has zero curvature, and the ray surface for the extraordinary wave has zero curvature only at cut-off $X = 1 \pm Y$ (trivial because $V \to \infty$) and at the upper hybrid frequency $X = 1 - Y^2$ (trivial because $V \to 0$).

5.3. For an electron plasma, there is an optic ray axis in the direction $\beta = 0$, so that the ray surfaces there have the form of two opposite cones with apices touching. Show that the wave normals make with the axis an angle Θ given by

$$\tan\Theta = \frac{\{P(1+Y)+1\}\{P(1-Y)+1\}(X-1)}{(P+1)\{P(1-Y^2-X)+1-X\}}$$

where

$$P = \pm\{(1-X)/(1-X-Y^2)\}^{\frac{1}{2}}.$$

(One method is to use equations (28), (11), (12) of Budden and Daniell, 1965). Alternatively it can be done by using (5.12), (5.33) with $\beta = 0$). Show in a similar way that when two ray surfaces cross on the plane $\beta = \frac{1}{2}\pi$, their wave normals make with the axis $\beta = 0$ an angle Θ given by

$$\cot^2\Theta = -\tfrac{1}{2} \pm \frac{Y^2 - 1 + X}{2(1-X)(1-Y^2)^{\frac{1}{2}}}.$$

5.4. Evaluate $(1/n)\,\mathrm{d}n/\mathrm{d}\Theta$ for the general collisionless plasma with ions included. Hence find the condition that $\mathrm{d}n/\mathrm{d}\Theta = 0$ when $\sin\Theta \neq 0$, $\cos\Theta \neq 0$.

5.5. Show that for a collisionless electron plasma at extremely low frequency ω, one of the values n of the refractive index is given by $n^2 \approx (\omega_N^2/\omega\omega_H)\sec\Theta$ where Θ is the angle between the wave normal and the superimposed magnetic field. Hence find the values of Θ for a given ray direction β, in the limit $\omega \to 0$. (Note that this is not realistic in practice because the ions have been ignored.)

5.6. In a homogeneous magnetoplasma a wave has ray velocity $V = c/(n\cos\alpha)$ and group velocity $\mathscr{U} = c/(n'\cos\alpha)$. ($\alpha$ and n' defined in (5.33) and (5.65) respectively.) Prove that $1/\mathscr{U} = \{(\partial/\partial\omega)(\omega/V)\}_\beta$ where the ray direction β is held constant for the differentiation. (Note that, when β is constant, both n and α change when ω changes.) Hence show that the two expressions $c/(n'\cos\alpha)$ and $|\partial\omega/\partial\boldsymbol{\kappa}|$ for $\mathscr{U}$ are the same.

5.7. Show that, for frequencies very close to cut-off, the angles Θ between the axis and the wave normal, and β between the axis and the ray, are related by $\tan\Theta = 2\tan\beta$.

5.8. Show that for a given ray direction β, when the frequency approaches a resonance frequency, $n'\cos\alpha \to \infty$ so that $\mathscr{U} \to 0$. (For the solution see Budden and Stott, 1980, § 4.3).

5.9. For a collisionless electron plasma, a family of refractive index surfaces is drawn for a sequence of values of X, with a common origin and axis. Prove that when $Y > 1$ the envelope of these surfaces intersects their common axis at an angle $\arctan\{2(Y-1)\}^{\frac{1}{2}}$.

5.10. For a collisionless electron plasma show that, for propagation with the wave normals parallel to the superimposed magnetic field, the two values of $n' = \partial(\omega n)/\partial\omega$ are $\{1-\frac{1}{2}XY(1+Y)^{-2}\}/\{1-X/(1+Y)\}^{-\frac{1}{2}}$ and the same expression with the sign of Y reversed. Show that the two values are equal when $X = \{2(3Y^2-1) \pm 2(1+Y^2)(2Y^4-2Y^2+1)^{\frac{1}{2}}\}/\{Y^2(3+Y^2)\}$. Show that this gives propagated waves (real n and n') only when $Y > 1$.

5.11. For longitudinal propagation in a collisionless electron plasma one of the refractive indices n is given by $n^2 = 1 - X/(1-Y)$. Show that the group refractive index n' is given by $nn' = 1 + \frac{1}{2}XY/(1-Y)^2$. Hence or otherwise show that for the whistler mode ($Y > 1$), when f_N is the plasma frequency and f_H is the electron gyrofrequency, n' has a minimum value when the frequency f satisfies

$$(f/f_H)^4 - (f/f_H)^3 - (f_N/f_H)^2\,(f/f_H - \tfrac{1}{4}) = 0.$$

Show that this gives $f/f_H \approx \frac{1}{4}$ when f_N/f_H is large, and that in all cases $f/f_H < \frac{1}{4}$.

5.12. Show that for an isotropic electron plasma the complex refractive index n and group refractive index n' satisfy $nn' = 1 + \frac{1}{2}\mathrm{i}XZ(1-\mathrm{i}Z)^{-2}$, Show also that $1/\mathrm{Re}(n) - \mathrm{Re}(n') = \frac{1}{8}XZ^2(3X-8)(2X-1)(1-X)^{-\frac{5}{2}} + \mathrm{O}(Z^3)$.